LBNL-3884E

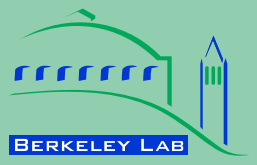

ERNEST ORLANDO LAWRENCE
BERKELEY NATIONAL LABORATORY

Implications of Wide-Area Geographic Diversity for Short-Term Variability of Solar Power

Andrew Mills and Ryan Wiser

Environmental Energy Technologies Division

September 2010

Download from http://eetd.lbl.gov/EA/EMP

The work described in this paper was funded by the U.S. Department of Energy (Office of Energy Efficiency and Renewable Energy and Office of Electricity Delivery and Energy Reliability) under Contract No. DE-AC02-05CH11231.

Disclaimer

LBNL-3884E

Implications of Wide-Area Geographic Diversity for Short-Term Variability of Solar Power

Prepared for the

Office of Energy Efficiency and Renewable Energy
Solar Energy Technologies Program
U.S. Department of Energy
Washington, D.C.

and the

Office of Electricity Delivery and Energy Reliability
Research & Development Division and
Permitting, Siting and Analysis Division
U.S. Department of Energy
Washington, D.C.

Principal Authors:

Andrew Mills and Ryan Wiser
Ernest Orlando Lawrence Berkeley National Laboratory

1 Cyclotron Road, MS 90R4000
Berkeley CA 94720-8136

September 2010

The work described in this report was funded by the Office of Energy Efficiency and Renewable Energy (Solar Energy Technologies Program) and by the Office of Electricity Delivery and Energy Reliability (Research & Development Division and Permitting, Siting and Analysis Division) of the U.S. Department of Energy under Contract No. DE-AC02-05CH11231.

Acknowledgments

The work described in this paper was funded by the U.S. Department of Energy (Office of Energy Efficiency and Renewable Energy, Solar Energy Technologies Program and Office of Electricity Delivery and Energy Reliability, Research & Development Division and Permitting, Siting and Analysis Division) under Contract No. DE-AC02-05CH11231. We would particularly like to thank Larry Mansueti, Gilbert Bindewald, Dan Ton, Charles Hemmeline, and Kevin Lynn (U.S. Department of Energy) for their support of this work. For guidance throughout this project we thank Abraham Ellis (Sandia National Laboratory), Ray George (National Renewable Energy Laboratory, NREL), Thomas Hoff (Clean Power Research), Benjamin Kroposki (NREL), Peter Larsen (LBNL), Michael Milligan (NREL), Mark O'Malley (University College Dublin), Dave Renne (NREL), Manajit Sengupta (NREL), Joshua Stein (Sandia), Thomas Stoffel (NREL), and Yih-huei Wan (NREL). Finally, for reviewing earlier versions of this report, we thank Mark Ahlstrom (WindLogics), Jay Apt (Carnegie Mellon University), Kevin Collins (FirstSolar), Joe Eto (LBNL), Hannele Holttinen (VTT Technical Research Centre of Finland), Sophie Pelland (Natural Resources Canada), and Jianhui Wang (Argonne National Laboratory). Of course, any remaining omissions or inaccuracies are our own.

Abstract

Worldwide interest in the deployment of photovoltaic generation (PV) is rapidly increasing. Operating experience with large PV plants, however, demonstrates that large, rapid changes in the output of PV plants are possible. Early studies of PV grid impacts suggested that short-term variability could be a potential limiting factor in deploying PV. Many of these early studies, however, lacked high-quality data from multiple sites to assess the costs and impacts of increasing PV penetration. As is well known for wind, accounting for the potential for geographic diversity can significantly reduce the magnitude of extreme changes in aggregated PV output, the resources required to accommodate that variability, and the potential costs of managing variability. We use measured 1-min solar insolation for 23 time-synchronized sites in the Southern Great Plains network of the Atmospheric Radiation Measurement program and wind speed data from 10 sites in the same network to characterize the variability of PV with different degrees of geographic diversity and to compare the variability of PV to the variability of similarly sited wind. The relative aggregate variability of PV plants sited in a dense 10×10 array with 20 km spacing is six times less than the variability of a single site for variability on time scales less than 15-min. We find in our analysis of PV and wind plants similarly sited in a 5×5 grid with 50 km spacing that the variability of PV is only slightly more than the variability of wind on time scales of 5-15 min. Over shorter and longer time scales the level of variability is nearly identical. Finally, we use a simple approximation method to estimate the cost of carrying additional reserves to manage sub-hourly variability. We conclude that the costs of managing the short-term variability of PV are dramatically reduced by geographic diversity and are not substantially different from the costs for managing the short-term variability of similarly sited wind in this region.

Contents

List of Figures

List of Tables

1 Introduction

Worldwide interest in the deployment of photovoltaic generation (PV), both distributed throughout the urban landscape and in large-scale plants, is rapidly increasing. PV plants as large as 60 MW are operating in Europe, while 500 MW PV plants are in various stages of development in the United States. Operating experience with large PV plants, however, demonstrates that large, rapid changes in the output of PV plants are possible. The output of multi-MW PV plants in the Southwest U.S., for example, are reported to change by more than 70% in five to ten minutes on partly-cloudy days (NERC, 2009). The reliable integration of generating plants with variable and uncertain output requires that power system operators have adequate resources to ensure a balance between the load and generation. The variability of PV output may create some concern about the ability of system operators to maintain this balance.

Early studies of the power system impacts of PV highlighted the rapid ramping of PV plants due to clouds, and the commensurate increased need for balancing resources, as a potential limiting factor in the grid penetration of PV. Many of these early studies, however, lacked high-quality data from multiple sites to assess the costs and impacts of increasing PV penetration. Similar concerns were raised some years ago regarding the variability of wind energy in studies that were often based on scaling the output of single wind turbines or anemometers to hypothetical large scale deployment (Wan and Parsons, 1993). More recent state-of-the-art studies of wind energy integration into the electric power system, however, have demonstrated the significant smoothing effect of geographic diversity, particularly with regards to rapid changes in the output of several interconnected wind plants. The lack of correlation between rapid changes in the output of different wind turbines reduces the variability of the aggregated wind output relative to the variability projected from simple scaling of the output of a single turbine (Farmer et al., 1980; Beyer et al., 1990; Grubb, 1991; McNerney and Richardson, 1992; Ernst et al., 1999; Persaud et al., 2000; Wan et al., 2003; Nanahara et al., 2004; Wan, 2005; Holttinen, 2005; Sorensen et al., 2007; Holttinen et al., 2009). A large body of experience with and analysis of wind energy demonstrates that this geographic smoothing over short time scales results in only a modest increase in balancing reserves required to manage the short-term variability of wind energy (Gross et al., 2006; Smith et al., 2007; Holttinen et al., 2009; Wiser and Bolinger, 2010).

The objective of this study is to assess the potential impact of the short-term variability of PV plants by exploring the short-term variability of PV output, the spatial and temporal scales of geographic diversity of PV, and the implications for the cost of managing the short time-scale, stochastic variability in the power system. Aside from the short-term variability impacts of PV, there are additional important considerations that we do not consider in the limited scope of this study. We do not evaluate the very-short time scale variability (<1-min) of PV which may affect power quality and may require careful evaluation in interconnection standards for PV. We do not consider the forecastability of PV and wind over multiple hours to days ahead and therefore do not include an assessment of the unit-commitment costs of PV and wind in this study (Tuohy et al., 2009; EnerNex Corp., 2009). We do not consider the avoided energy costs of PV (or the *energy value* of PV) and the

contribution of PV to long-term planning reliability or resource adequacy (or the *capacity value* of PV). We also do not consider the flexibility of the conventional generation system over multiple hour periods. We therefore do not assess the potential for curtailment of PV at high penetrations due to minimum generation constraints (Denholm and Margolis, 2007) or for operational cost implications of large multiple hour ramps with systems that have inflexible conventional generators. Finally we do not consider the potential value of PV for transmission expansion deferral or the potential need to increase investments in transmission/distribution infrastructure in areas where PV production exceeds the local load. These broader issues are discussed in more detail elsewhere (U.S. DOE, Forthcoming).

To asses the potential impact of short-term variability of PV, the characteristics of short-term variability of PV are compared to the characteristics of wind in a specific region of the United States. As explained in further detail in the report, the data used in this analysis are measured 1-min solar insolation and estimated 1-min clear sky insolation for 23 time-synchronized sites in the Southern Great Plains network of the Atmospheric Radiation Measurement program. Wind speed data from 10 of the sites in the same network are converted into estimated wind power output to compare the variability of PV and wind. Variability across different time scales is analyzed by calculating the step changes from one averaging interval to the next over different averaging intervals from 1-min to three hours. Diversity across these different time scales is measured by the degree of correlation of variability as a function of distance between sites. The results of this analysis demonstrate that, at individual sites, PV is more variable than wind for sub-hourly time scales, but that the distances between sites required to obtain diversity and therefore smooth the output for sub-hourly variability are slightly less for PV than for wind. Overall, for similarly sited PV and wind plants sited in a 5×5 grid with 50 km spacing, we find that the variability of PV is slightly more than wind, particularly for variability on time scales of 5-15 min. Finally, we use a simple approximation method to estimate the cost of carrying additional reserves to manage short-term variability. We conclude that the costs of managing the short-term variability of geographically distributed PV plants are not substantially different from the modest costs to manage the short-term variability of similarly sited and geographically distributed wind in this region.

The remainder of this paper is organized as follows:

- Section 2 provides an overview of the short-term variability impacts of PV plants and the potential economic consequences of measures to maintain the same level of reliability with and without PV.
- Section 3 reviews the methods used to quantify the variability of PV and wind while accounting for the impacts of geographic diversity and the methods used to estimate the costs of managing this variability.
- Section 4 summarizes the data sources used to quantify the short-term variability of PV and wind using time-synchronized data from multiple sites in the same region.

- Section 5 presents the results from the examination of the variability of PV on different time scales and at different levels of geographic diversity.
- Section 6 summarizes a simple analysis of the potential cost implications of the variability of PV compared to wind.
- Section 7 presents our conclusion that for a particular arrangement of similarly sited PV and wind, the variability of PV is only slightly greater than the variability of wind for sub-hourly time scales. We therefore expect that the costs to manage short-term variability of PV will not be substantially different from the costs to manage the short-term variability of wind energy in this region.

2 Power System Impacts Due to Short-term Variability of PV Plants

The short-term variability of PV generation will impact the power system in a variety of ways. Our analysis focuses only on the operational integration impacts of stochastic (i.e. cloud-induced rather than deterministic changes due to the movement of the sun) PV variability over short time scales. Namely, our analysis is focused on the need for power system operators to maintain a short-term balance between generation and loads.

The North American Electric Reliability Corporation (NERC) sets mandatory reliability standards for balancing authorities within the U.S. Balancing authorities (BAs) are the entities responsible for maintaining a balance between load, generation, and scheduled imports and exports across transmission lines that tie multiple balancing authorities together. NERC reliability standards for generation and demand balancing require that each BA maintain adequate balancing performance as measured by a 12-month rolling average of the 1-min contributions of that BA to interconnection-wide frequency deviations (Control Performance Standard 1 or CPS1), a 1-month count of the number of 10-min periods for which adequate balance was maintained within the period (CPS2), and the ability to recover from the single largest contingency[1] within 15 minutes (Disturbance Control Standard, or DCS) (NERC, 2008). Although it is not a reliability requirement, BAs in the U.S. schedule power transfers with other BAs generally using hourly schedules. The BA is responsible for maintaining the scheduled power transfers irrespective of changes in generation or load (generally called imbalances or hour-ahead forecast errors). BAs that use hourly schedules therefore must also have sufficient resources to maintain the schedules in order to meet the NERC standards. Numerous initiatives are underway in North America to enable shorter scheduling periods, some as short as five minutes, between BAs to reduce the burden on BAs to manage imbalances.

Though NERC enforces these balancing standards, it does not specify *how* a BA must meet the standards. The rules and practices used to maintain reliability therefore vary from

[1] A typical contingency might include the loss of a tie-line to another balancing authority or a large power plant tripping off-line due to a forced outage.

one area to another. In general, system operators rely on several resources and methods to maintain reliability, including:

- Holding dispatchable resources in reserve. Operating reserves are used to recover from the near instantaneous change in the system due to a large contingency. Regulating reserves are used to rapidly respond to changes in the balance between load and generation on the time scale of minutes. BAs may also hold resources in reserve to be available when inaccurate forecasts or schedules leave insufficient resources available to follow changes in the load minus the actual output of any variable generators, or the *net-load*. Reserves are generally composed of spinning reserves that are online and synchronized with the grid (and following an automatic generation control (AGC) signal in the case of regulation reserves) or non-spinning reserves that are available to provide response with short notice.

- Economic dispatch or load following to adjust the output of units to follow longer minutes-to-hour trends in the net-load.

- Unit-commitment to schedule units to be available and on-line in the hours to days ahead time scale.

The additional variability and uncertainty introduced by PV plants will, to some degree, increase the use of these resources and methods to maintain balance, which will impose costs to the power system. Additional uncertainty and variability over time scales shorter than the time it takes to start and synchronize fast-start units, for instance, must be met by balancing reserves from spinning resources. An increase in spinning resources held in reserve leads to more units dispatched to "part load" levels, which leads to an efficiency penalty and higher costs than dispatching units to optimal set points (Mills et al., 2009b). Increased ramps in the net-load over the time scale of the economic dispatch may also require out-of-merit order dispatch whereby a fast ramping, but higher cost, unit is dispatched to produce more power while a slow ramping, but lower cost, unit is slowly moved to its higher set point (Kirby and Milligan, 2008).

To some extent, previous studies have evaluated the balancing resources required to accommodate the short-term variability of PV. Unlike the extensive body of work on the operational integration impacts of wind, however, these (often-dated) studies generally lack high-time resolution PV data from multiple sites. Many of the conclusions are instead based on scaling PV data from single sites or simple cloud models (Table 1). These studies often conclude that the economic value of PV is significantly reduced at increasing levels of PV penetration due to the additional need for reserves or that the high variability of PV and the limited ramp rates of conventional generation limit the feasible penetration of PV. The conclusions of these studies are questionable due to the lack of high time-resolution data from multiple PV sites. Studies that have evaluated sub-hourly PV data from multiple sites, on the other hand, do not separate the impacts of PV from the impacts of much larger quantities of wind and solar thermal plants (Piwko et al., 2007, 2010).

System operators only need to balance the variability of the load net the aggregated output of PV sites in the balancing area (while respecting transmission capacity limits).

Table 1: Sample of PV operational integration studies that focus on short-term variability[a]

Reference	PV Variability	Conclusions
Lee and Yamayee (1981)	100% change in 10-min assumed for PV	Dispatch and operating reserve penalties for PV can eliminate economic value.
Chalmers et al. (1985)	Simple uniform cloud model generates worst case ramps	Variability exceeds ramp-rate capability of on-line generation at low PV penetration.
Chowdhury and Rahman (1988)	Simulated 10-min data for single, 750 MW PV plant	Out-of-merit order dispatch due to limited ramp rates of thermal units can eliminate economic value of PV.
Jewell and Unruh (1990)	Cumulus cloud model and synthetic 1-min PV data assumed to have different magnitude fluctuations	PV penetration limited by ramp-rates of dispatchable generation. Limit is relaxed as PV is increasingly dispersed.
Bouzguenda and Rahman (1993)	Scaled 10-min data from single 20 kW PV plant	PV penetration limited by ramp-rates of dispatchable generation.
Asano et al. (1996)	Scaled 10-sec data from a single location	PV increases required capacity and ramp-rates of units used to balance 5-30 min variability.
Piwko et al. (2007)	15-min PV production data from multiple sites overlaid with synthesized short-term data assumed to be uncorrelated between sites	Operational integration impacts are modest.[b]
Piwko et al. (2010)	Hourly satellite-derived PV production overlaid with synthesized 10-min PV production data from multiple sites	Operational integration impacts are modest.[b]

a - EnerNex Corp. (2009) evaluates unit commitment costs but does not address short-term variability

b - Impacts of PV were not separately identified in scenarios with much more wind and solar thermal

The degree to which PV increases the demand for resources to balance the net load therefore depends on the amount of smoothing offered by geographic diversity.

Previous research demonstrates that smoothing from geographic diversity for solar does occur. Jewell and Ramakumar (1987) and Kern and Russell (1988) develop cloud models to estimate the smoothing effect of geographic diversity. Jewell and Ramakumar (1987) consider regions ranging from 10 km^2 to 100,000 km^2, while Kern and Russell (1988) consider an area of 0.2 km^2 (50-acres). Wiemken et al. (2001) use data from actual PV sites in Germany to demonstrate that 5-min ramps in normalized PV power[2] at one site may exceed +/-50% but that 5-min ramps in the normalized PV power from 100 PV sites spread throughout the country[3] never exceed +/- 5%. Results from Curtright and Apt (2008) based on three PV sites in Arizona indicate that 10-min step-changes in output can exceed 60% of PV capacity at individual sites, but that the maximum of the aggregate of three sites is reduced.[4] Otani et al. (1997) demonstrate that the variability of sub-hourly irradiance even within a small area of 4 km $\times$ 4 km can be reduced from geographic diversity. Kawasaki et al. (2006) similarly analyze the smoothing effect within a small 4 km $\times$ 4 km network of irradiance sensors and conclude that the smoothing effect is most effective during times when the irradiance variability is most severe—particularly days characterized as partly cloudy. Murata et al. (2009) develop and validate a method for estimating the variability of PV plants dispersed over a wide area[5] that is very similar to the methods we use in the next section (and to methods used for wind by Ilex Energy Consulting Ltd et al. (2004) and Holttinen (2005)). Their analysis shows that the aggregate variability of PV plants sited over a wide area depends on the correlation of the variability between plants. The correlation of variability, in turn, is a function both of the time scale and distance between plants. Variability is less correlated for plants that are further apart and for variability over shorter time scales.[6]

[2]Normalized PV power is measured PV power divided by the installed capacity of PV.

[3]The area covered by the sites is about 600 km $\times$ 750 km, or about 450,000 km^2.

[4]In contrast to the other studies reviewed in this paragraph, Curtright and Apt (2008) state that their PV data "imply that site diversity over a $\sim$280 km range does not dampen PV intermittency sufficiently to eliminate the need for substantial firm power or dispatchable demand response. The high correlation between geographically dispersed arrays may indicate that high, widespread clouds are responsible for a portion of the intermittency." These results do not agree with the conclusions from the other literature cited in this paragraph because Curtright and Apt (2008) (1) consider only a limited number of sites (three) and (2) their calculation of correlation coefficients between the three sites uses the full time-series across all time scales rather than isolating the variability across particular shorter time scales. The high correlation coefficients (0.5-0.73) they find between distant sites (110 km to 290 km apart) are in part due to the correlated, deterministic change in the position of the sun at the three sites and changes in insolation over multiple hour time scales. Our results, presented in later sections, find diversity over multiple sites within a $\sim$280 km range can dramatically reduce variability over sub-hourly time scales.

[5]They consider 52 sites across the country of Japan from 2 km to 923 km apart.

[6]The results of the study by Murata et al. (2009) are unfortunately not directly comparable to our results, however, because they do not separate changes in PV output that occur from clouds from the deterministic changes that occur due to changes in the position of the sun. As a result, variability over time scales longer than 20-min or so in their results do not drop to zero with increasing distance due in part to the deterministic changes in the position of the sun. As explained in the next section, our analysis separates this deterministic component from the stochastic component due to the movement of clouds through the use of the clear sky index.

Interestingly, Murata et al. (2009) find nearly zero correlation between 1-min and 5-min fluctuations at all distances between sites, even distances as close as 2 and 9 km apart, respectively. Even different inverters within a single 13.2 MW PV plant in Nevada can have very low correlations in 1-min changes on a highly variable day (Mills et al., 2009a). Hoff and Perez (2010) develop a simple model to predict the relative variability of a fleet of PV plants to the variability of individual plants using the number of plants and a parameter they define as the dispersion factor. The dispersion factor is based on the ratio of the time required for a cloud to pass over the entire fleet of PV plants to the time scale of interest. The average variability of the fleet over the time scale of interest is estimated to equal only $1/\sqrt{N}$ of the variability of a single site if the dispersion factor is larger than the number of plants in the fleet, but approaches the variability at a single site as the dispersion factor decreases to one. Hoff and Perez (2010) predict that the average variability of the fleet reaches a minimum when the dispersion factor is equal to the number of plants in the fleet.

Overall, the clear conclusion from this body of previous research is that with "enough" geographic diversity the sub-hourly variability due to passing clouds can be reduced to the point that it is negligible relative to the more deterministic variability due to the changing position of the sun in the sky. It is not necessarily clear how dispersed PV will be in the future, however. Siting considerations including available land or rooftop area or available transmission capacity may naturally lead to a high degree of dispersion. On the other hand, if plants would naturally be more densely sited, obtaining more geographic diversity will introduce additional costs. Increasing the spacing between PV plants may require additional transmission capacity or increased transmission losses. Similarly, increasing the spacing between plants may require moving some plants out of the highest quality solar resource areas. Since the quality of the solar resource dictates the capacity factor of a PV plant, a reduction in the quality of the solar resource will increase the generation cost of the repositioned PV. Also breaking up a large PV plant into smaller dispersed PV plants may forgo economies of scale available to the larger PV plant.

The tradeoff between the costs to increase geographic dispersion and the benefits of the reduced variability seen by the system operators is a complex problem that will generally be site and system specific. Instead of determining the best deployment of PV plants, we therefore only focus on understanding key drivers of this tradeoff for both PV and wind: the characteristics of variability and the spatial and temporal scales of geographic diversity. Specifically, we investigate the short-term variability of similarly sited PV and wind plants.

3 Methodology

3.1 Estimation of the Variability from Dispersed Photovoltaic Plants

The operational integration impacts of PV plants will depend on the characteristics of the variability over various time scales. Variability over short time scales, for example a rapid change in the net-load that must be met by conventional generation, is relatively more challenging and more expensive to accommodate than similar sized changes over longer time

periods.

A common method for characterizing the variability of a resource over different time scales is to calculate the "deltas" or "step changes", which refers to the difference in the output of a plant from one averaging interval to another. The duration of the averaging interval is $\bar{t}$. Given minute by minute output data at a single site, P_1, a step change at a single site with a sixty minute averaging interval, for example, is calculated as:

$$\Delta P_1^{\overline{60}}(t) = P_1^{\overline{60}}(t) - P_1^{\overline{60}}(t-60) = \left(\frac{1}{60}\sum_{i=0}^{59} P_1(t+i)\right) - \left(\frac{1}{60}\sum_{i=-60}^{-1} P_1(t+i)\right) \quad (1)$$

The overall average variability of the resource at a single point over an averaging interval can then be characterized by the standard deviation of the step changes over a long observation period or by some percentile of the step changes. A common metric is the 99.7^{th} percentile (Holttinen et al., 2008), which corresponds to three standard deviations from the mean for a normally distributed random variable.[7] The standard deviation of the step changes with a sixty minute averaging interval at a single site, $\sigma_{\Delta P_1}^{\overline{60}}$ is:

$$\sigma_{\Delta P_1}^{\overline{60}} = \sqrt{\mathrm{Var}\left(\Delta P_1^{\overline{60}}\right)} \quad (2)$$

The 99.7^{th} percentile may be more or less than three standard deviations from the mean depending on the shape of the distribution of the step changes. A distribution with relatively "fat tails" will have a 99.7^{th} percentile that exceeds three standard deviations. We follow nomenclature and definitions slightly different from Murata et al. (2009) and refer to the ratio of the 99.7^{th} percentile to the standard deviation of the step changes over different averaging intervals as $\kappa_{3\sigma}$:

$$\kappa_{3\sigma}^{\bar{t}} = \frac{99.7^{\text{th}} \text{ percentile of } |\Delta P_1^{\bar{t}}|}{\sigma_{\Delta P_1}^{\bar{t}}} \quad (3)$$

For maintaining compliance with NERC reliability standards, however, system operators need only to balance the load net of all generation rather than the output of individual

[7] There are, of course, a multitude of different ways to characterize variability over different time scales. We choose to use the standard deviation and 99.7^{th} percentile of step changes from data averaged over different time-averaging periods because this method is commonly used in wind integration studies. Murata et al. (2009) apply a slightly different metric based on the ramps generated using different lag times (rather than data averaging times). Woyte et al. (2007) characterize variability over different time scales using a localized spectral analysis based on wavelets. This method isolates the magnitude of the fluctuations that occur according to their persistence time scale. Both of these methods are perhaps more mathematically accurate and concise relative to the manner used in the present study, but the method used here is often used in practice. Curtright and Apt (2008) use spectral analysis to characterize the variability of PV over different time scales. In contrast to the localized spectral analysis employed by Woyte et al. (2007), however, the approach used by Curtright and Apt (2008) implicitly assumes that fluctuations across all time scales are periodic. A comprehensive review of methods used to characterize variations in solar insolation at a single site is available from Tovar-Pescador (2008).

plants. More important than the variability of a single variable generation plant, therefore, is the variability of the sum of all variable generation plants. N plants each with an output of $P_i(t)$ leads to an aggregate output, $P(t)$, of:

$$P(t) = P_1(t) + P_2(t) + P_3(t) + P_4(t) + ... + P_n(t) \tag{4}$$

Using the standard deviation of the step changes metric, the total variability of the aggregate of all PV plants for a particular averaging interval, $\sigma^{\bar{t}}_{\Delta P}$, is:

$$\sigma^{\bar{t}}_{\Delta P} = \sqrt{\text{Var}\left(\Delta P^{\bar{t}}\right)} = \sqrt{\sum_{i=1}^{N}\sum_{j=1}^{N}\text{Cov}\left(\Delta P_i^{\bar{t}}, \Delta P_j^{\bar{t}}\right)} \tag{5}$$

The role of geographic diversity is to reduce the variability of the aggregate of multiple plants relative to scaling the output of a single plant (even though the absolute level of variability of N plants in aggregate will be larger than the absolute level of variability at an individual site). This benefit is called a "diversity factor" (Farmer et al., 1980), a "space filter" (Healey, 1984), an "equivalent filter" (Nanahara et al., 2004), or as we call it, a "diversity filter." As mentioned in the introduction, the benefit of geographic diversity has been analyzed in detail for wind energy. For our purposes, we define a diversity filter as a process that changes the variability of multiple sites relative to summing the variability of each site independently. The impact of diversity is demonstrated by the ratio of the aggregated variability of all sites to the sum of the variability of each individual site.

$$\text{Diversity Filter} = D^{\bar{t}} = \frac{\sigma^{\bar{t}}_{\Delta P}}{\sum_{i=1}^{N}\sigma^{\bar{t}}_{\Delta P_i}} \tag{6}$$

For purposes of simplification, if it is assumed that all N plants are similar in that they have the same variability, then the diversity filter over different time scales reduces to:

$$D^{\bar{t}} = \frac{\left(\sigma^{\bar{t}}_{\Delta P}/N\right)}{\sigma^{\bar{t}}_{\Delta P_1}} = \frac{1}{N}\sqrt{\sum_{i=1}^{N}\sum_{j=1}^{N}\rho^{\bar{t}}\left(\Delta P_i^{\bar{t}}, \Delta P_j^{\bar{t}}\right)} \tag{7}$$

Where $\rho^{\bar{t}}\left(\Delta P_i^{\bar{t}}, \Delta P_j^{\bar{t}}\right)$ is the correlation coefficient of the $\bar{t}$-min step changes between sites i and j. The diversity filter (the ratio of the variability of PV at the system level to the variability of PV at all sites individually) therefore depends on the correlation of the step changes for each time scale, which is a function of both the spatial and temporal scales. For sites located very close to each other, such that they are perfectly correlated over a time scale of $\bar{t}$ (and therefore $\rho^{\bar{t}} = 1$), the diversity filter is equal to 1: the variability at the system level is equivalent to the sum of the variability of PV at all sites individually. When plants are sited such that they are perfectly uncorrelated over a time scale of $\bar{t}$ (and therefore $\rho^{\bar{t}} = 0$) the diversity filter is equal to $\frac{1}{\sqrt{N}}$: the variability at the system level is $\sqrt{N}$ times the variability at a single site (again assuming all sites have similar size and variability characteristics).

Based on relationships developed by Nanahara et al. (2004) and Glasbey et al. (2001), and results from Murata et al. (2009), it is expected that the correlation of deltas between two sites will decrease exponentially with increasing distance, d_{ij}, and will similarly decrease with shorter averaging intervals, $\bar{t}$. A functional form that captures both this spatial and temporal behavior of correlation is:

$$\rho^{\bar{t}}\left(\Delta P_i^{\bar{t}}, \Delta P_j^{\bar{t}}\right) = \frac{1}{2}\left(e^{-\frac{C_1}{\bar{t}}d_{ij}^{b1}} + e^{-\frac{C_2}{\bar{t}}d_{ij}^{b2}}\right) \tag{8}$$

Where C_1, C_2, b_1 and b_2 are constant parameters that can be estimated from a fit to solar data in a particular region. At zero distance the correlation is one and as the distance between sites increases the correlation reduces to zero. Similarly, for very long time scales the correlation increases to one and over very short time scales falls to zero.

Assuming this particular functional form and that all plants are similar in their ramping characteristics and size allows the diversity filter to be specified in terms of the distance between PV plants and two model constants.

$$D_{\Delta}^{\bar{t}} = \frac{1}{N}\sqrt{\sum_{i=1}^{N}\sum_{j=1}^{N}\left(\frac{1}{2}\left(e^{-\frac{C_1}{\bar{t}}d_{ij}^{b1}} + e^{-\frac{C_2}{\bar{t}}d_{ij}^{b2}}\right)\right)} \tag{9}$$

According to this formula and the assumption that all plants are similarly sized and have similar variability characteristics, the variability of all plants aggregated to the system level can be determined based on the variability of a PV plant at a single site, the model constants, and the location of each PV plant.

For PV, rapid output changes are largely driven by fast moving clouds. PV output also changes based on diurnal cycles of the sun, but this variability can be perfectly forecasted. The variability due to changes in the position of the sun can therefore be evaluated by system operators without consideration of geographic diversity. Because of the relative lack of understanding of the short-term variability due to fast moving clouds we focus on the stochastic component of the variability of PV output. This stochastic component due to cloud movement can be separated from the deterministic component due to changes in the position of the sun in the sky by focusing only on the clear sky index, $k(t)$, in place of the overall change in power output, $P(t)$. The clear sky index is the ratio of the actual global insolation measured at the site to the global insolation expected if the sky were clear (Figure 1). Since PV plant output is generally proportional to solar insolation, the variability of the clear sky index is similar to the variability of the ratio of actual PV plant output to PV plant output if the sky were clear. The stochastic variability in solar insolation is not exactly equivalent to the stochastic variability in actual PV plants due to "within-plant" smoothing that can occur relative to variability of insolation at a point (Mills et al., 2009a), changes in PV plant efficiency with temperature, PV tracking systems, and diverse PV panel orientations other than horizontal for non-tracking PV systems.[8] We focus on the

[8]Mills et al. (2009a) summarize comparisons between variability of point insolation measurements and PV plant output. Within-plant smoothing reduces variability on time scales shorter than about 10-min for a 13.2 MW PV plant.

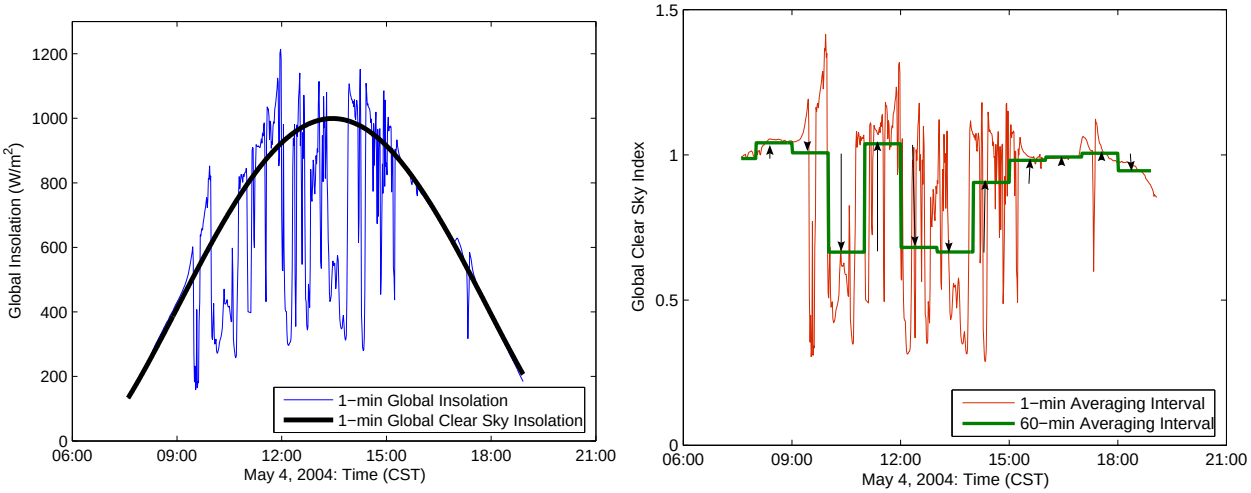

(a) Example of 1-min global insolation and global clear sky insolation on a partly cloudy day

(b) Example of 1-min global clear sky index, 60-min average of the clear sky index, and arrows representing magnitude and direction of 60-min deltas

Figure 1

variability of the clear sky index from insolation measurements rather than the variability of the clear sky index from actual PV plants for the bulk of this study because of the relative higher quality of the insolation dataset available at the time of this study. The variability, particularly over shorter time scales, in our results will most likely provide an upper bound to the stochastic variability expected from actual PV plants.

3.2 Estimation of the Cost to Manage Short-Term Variability at the System Level

Determining the cost of managing sub-hourly variability is a complex problem that is generally evaluated through detailed integration studies. Without performing a detailed integration study we still want to understand in general terms the relative difference in cost between managing variability at a single site and variability estimated for an aggregate of multiple sites. Similarly, we want to understand the cost of managing short-term variability of PV relative to the more-well-known cost of managing the stochastic short-term variability of wind. Based on these broad objectives, we provide a simple estimate of the costs to manage short-term variability that is largely based on methods and assumptions from Farmer et al. (1980), Grubb (1991), Milborrow (2001), Wan (2005), and EnerNex Corp. and Windlogics Inc. (2006). These simple estimates are only meant to illustrate relative changes in costs; the cost impact of short-term variability should in the future be evaluated with more detailed methods.

To estimate the costs of managing sub-hourly variability we make the following simplifying assumptions:

- Only the net of the variability of load and variable generation is managed by the system operator.
- The incremental variability above the variability of the load is managed with additional balancing reserves.
- The capacity of the variable generation added is assumed to have a nameplate total that is 10% of the peak load.
- As a proxy for resources required to maintain a balance between load and generation, we characterize the additional variability on different time scales using the following deltas:
  - As a proxy for the NERC CPS1 standard, we use the 1-min deltas
  - As a proxy for the NERC CPS2 standard, we use the 10-min deltas
  - As a proxy for the imbalance or hour ahead forecast error we use the 60-min deltas[9]
- Over these short time scales we assume that load deltas are uncorrelated with the deltas from the variable generators. The variance of the net load deltas is therefore assumed to be the sum of the variance of the load deltas and the variance of the variable generator deltas.[10]
- We assume that the variability from the 1-min and 10-min deltas can only be met with resources that are spinning, or on-line and synchronized with the grid.

[9]Our use of the deltas as a proxy for the requirements to manage variability on different time scales follows approaches used in other detailed integration studies. The authors of the 2006 Minnesota Wind Integration Study estimate the increase in sub-hourly reserves for wind based on the 1-min deltas (regulation requirement), the 5-min deltas (load following requirement), and the 60-min deltas (operating reserve margin to cover forecast error using persistence forecast) (EnerNex Corp. and Windlogics Inc., 2006). The wind deltas are combined with the deltas from load to estimate the increase in the total balancing reserves in high wind scenarios relative to a base scenario. The authors of a 2004 study of the balancing reserves required to manage wind in the Irish system (Ilex Energy Consulting Ltd et al., 2004) based reserve requirements on the 1.25 min deltas (fast reserves), 30-min deltas (slow reserves), and 1-hour deltas (replacement reserves). The wind deltas are combined with the deltas from the load to estimate the increase in total balancing reserves at various levels of wind penetration using an algorithm similar to one presented by Doherty and O'Malley (2005). An earlier study of the costs of accommodating renewables in the UK used 30-min deltas (response) and 4-hour deltas (reserve) to estimate the balancing costs for wind. The 4-hour reserve was assumed to be met with a combination of standing reserve and spinning reserve, depending on the cost tradeoffs between part-load efficiencies for spinning reserve and start-up costs for standing reserve (Ilex Energy Consulting Ltd and Strbac, 2002).

[10]The 60-min variable generation and load deltas are likely to be correlated to some degree. The stochastic changes in insolation due to clouds, as captured by the clear sky index, however, are less likely to be correlated with changes in load than the changes in total solar insolation and load. Either way, we do not use time-synchronized load and variable generation data to account for correlation between generation and load deltas in our simple estimates. More detailed evaluations of the costs of managing short-term variability for a specific load should account for the potential correlation of generation and load over the 60-min time-scale, but the correlation is not expected to be significant.

- The amount of spinning reserves required to manage the 1-min and 10-min deltas is assumed to equal three times the standard deviation of the net load deltas. While we explore the shape of the non-normal distributions of the deltas, the general form of Eq. 7 does not provide information of how the shape of the distribution changes with the aggregation of multiple sites. In addition, without actual 1-min time-synchronized load data we do not know how the shape of the distribution of the net-load deltas will compare to the shape of the distribution of the variable generation deltas and load deltas. We therefore ignore the potential non-normal distributions of the net-load for the purpose of a simple estimation of costs. Future work in specific regions should directly evaluate the shape of the distribution of the net-load deltas.

- We assume that the variability from the 60-min deltas can be met with a combination of spinning and non-spinning resources. The amount of spinning reserves to manage the 60-min deltas is assumed to be half of the standard deviation of the 60-min deltas. Deltas larger than half of the standard deviation of the 60-min deltas are assumed to be met by deploying non-spinning resources.

- We assume that resources required to manage the 1-min, 10-min, and 60-min deltas are held in reserve and therefore cannot simultaneously also be used to meet the peak net load. The additional reserve requirement is therefore met with resources that cannot also provide capacity. We therefore assume that there is an opportunity cost of capacity associated with increasing these reserves.[11]

- The standard deviation of the deltas is assumed to be constant throughout the year for load and wind deltas. For PV deltas we examine two cases:

  - The standard deviation of the PV deltas is assumed to be constant and proportional to the standard deviation of the deltas from the clear sky index. For example, if the standard deviation of the clear sky index deltas is 0.1 then the standard deviation of the PV deltas is assumed to be 0.1 times the nameplate capacity of the installed PV.
  - The standard deviation of the PV deltas is assumed to change throughout the year in proportion to the clear sky insolation expected for any hour. Following the previous example, if the standard deviation of the clear sky index deltas is 0.1 then the standard deviation of the PV deltas is assumed to be 0.1 times the amount of power that would be produced by the PV plants if the sky were clear in any particular hour. This assumption allows the amount of reserves procured to manage PV variability to change with the position of the sun.[12]

[11] Note that the assumption that resources are held in reserve to meet 60-min deltas and that there is an opportunity cost of capacity for these resources is driven by hourly scheduling periods between BAs. The opportunity cost of capacity would be reduced if the solar and wind resources were integrated into BAs that have shorter scheduling periods (Kirby and Milligan, 2008, 2009).

[12] In this case no reserves are held to manage short-term variability of solar in the middle of the night when the clear sky insolation is zero. Similarly, fewer reserves are held during winter mornings with low clear sky

  - In either case, the opportunity cost of capacity is based on the peak reserve requirement and is not assumed to change depending on whether reserves are constant throughout the year or if they change with the position of the sun.

- The cost of spinning reserves is assumed to be based on an efficiency penalty for the marginal plant that is part-loaded to provide spinning reserves.

- The cost of non-spinning reserves is assumed to be based on the higher cost of energy from a quick starting plant that provides non-spinning reserve relative to the cost of energy from the marginal plant that would have otherwise been used.

Additional details and the equations used to estimate the additional cost of managing reserves are included in Appendix A.

3.3 Numerical Assumptions

In addition to the methodological assumptions, several numerical assumptions are required to estimate the cost of additional reserves to manage additional short-term variability. The assumptions used are listed in Table 2.

In the following sections we start by exploring the variability of PV at individual sites. We then evaluate the correlation of deltas between geographically dispersed sites and use real 1-min insolation data from multiple time-synchronized sites to develop the constants for Eq. 8. We then demonstrate the effectiveness of the diversity filter for an array of sites, and use a similar approach to compare the variability of an array of similarly sited solar and wind sites. Finally, we estimate the increased costs associated with managing the sub-hourly variability of solar and wind. Before presenting these results, however, Section 4 discusses the data used in this analysis.

4 Data

We explore the short-term variability of PV across multiple time scales at a single site by calculating the deltas in the clear sky index across an entire year. Variability is characterized by the standard deviation of the deltas, the shape of the distribution of the deltas, and the magnitude of the 99.7^{th} percentile of the deltas. Then, using time-synchronized data from multiple sites we examine the correlation of deltas between sites that are at varying distances from one another.

The primary data required for this analysis are high time resolution solar and wind data for multiple time-synchronized sites covering a broad geographic region. The only readily available U.S. dataset that fit this need was one that contains historic data from the Atmospheric Radiation Measurement (ARM) Program at the Southern Great Plains (SGP)

insolation than the reserves held in during summer afternoons when the clear sky insolation is at its peak. For the same type of clouds, the aggregate variability will be less if the clouds pass on a winter morning than if they pass during a summer afternoon.

Table 2: Numerical assumptions to estimate cost of additional reserves

Assumption	Value
Efficiency penalty of part loaded marginal plant, η	15%
Full-load variable cost of marginal plant, c_m	\$55/MWh
Variable cost of standing plant, c_g	\$85/MWh
Fixed cost of capacity, FC_p	\$100/kW-yr
Standard deviation of 1-min load deltas[a]	0.3% of peak
Standard deviation of 10-min load deltas	0.8% of peak
Standard deviation of 60-min load deltas	3.7% of peak
Multiple of st. dev. of deltas kept in reserve, κ	3
Multiple of st. dev. of 1-10 min deltas from spinning resources, $\gamma_{1,10}$	3
Multiple of st. dev. of 60 min deltas from spinning resources, γ_{60}	0.5
Capacity factor of solar, CF_S	20%
Capacity factor of wind, CF_W	30%

a - The load deltas are illustrative values from a Minnesota utility with a peak load of 6,000 MW (Wan, 2005)

network.[13] The solar data are 1-min averaged global, direct, and clear sky insolation from 23 instrument sites[14] from 2004. The sites are located 20 km to 440 km apart and are located in the states of Oklahoma and Kansas. Data on clear sky insolation and the cosine of the solar zenith angle data are provided with the SGP dataset. We use these data to calculate the clear sky index at each point measurement, $k_i(t)$, as the ratio of the measured insolation to the clear sky insolation. To avoid potential problems with calculating the clear sky index when the sun is near the horizon and clear sky insolation is very low, we only calculate the clear sky index for periods when the cosine of the solar zenith angle exceeds 0.15.

The SGP dataset also includes 1-min averaged wind speed data at 10 m from 15 instrument sites[15] in the SGP network. The wind speed data were extrapolated to the typical hub height of wind turbines, 80 m, using a simple $1/7^{th}$ power law extrapolation.[16] The

[13]Gaps in the time-series data were filled using tools provided by the ARM program. The data collected from the SGP site was run through a program called "nc fill" as part of the ARM NetCDF Tool Suite. The option was set to use linear interpolation to fill gaps in the data sets. We synchronized the 23 datasets by removing any data points that did not simultaneously occur at all sites in the network. Aside from the quality control provided by the ARM Program, no other additional cleaning or error checking procedures were performed on the data.

[14]The 23 sites with solar data are C1,E1-13, E15, E16, E18-22, E24, and E27.

[15]The 15 sites with wind data are E1, E3-9, E11, E13, E15, E20, E21, E24, and E27.

[16]The power law extrapolation is $u_{80} = u_{10}(80m/10m)^{\frac{1}{7}}$ where u_{80} is the extrapolated wind speed at 80 m above the ground and u_{10} is the measured wind speed 10 m above the ground. Wind variability

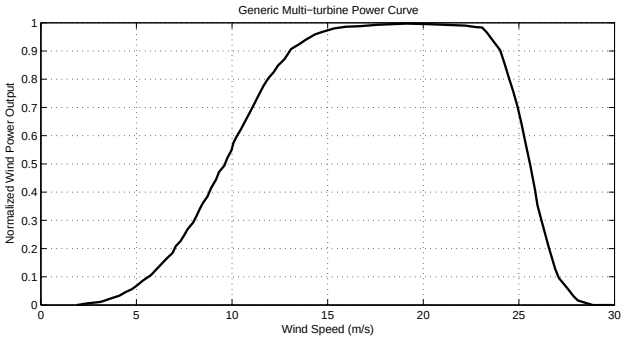

Figure 2: Generic multi-turbine power curve used to convert hub-height wind speed to wind power from Holttinen (2005).

wind speed data were then converted into wind power output using a multi-turbine power curve,[17] recreated in Figure 2 (Holttinen, 2005). Wind speed data from five of the 15 sites showed very low annual capacity factors (below 20%) and were therefore excluded from our assessment of wind variability.[18]

5 Results

5.1 Deltas at Individual Sites

The anecdotes of extreme deltas from PV plants and the conclusions from many of the previous solar integration studies described in Table 1 are based, in large measure, on data from single sites. In this section we examine the deltas at individual sites within the SGP network.

over short time scales may be greater at 10m than it is at 80m due to turbulence. We do not correct for potential changes in variability with height and our results may therefore overestimate the variability of wind, particularly over time-scales shorter than 10-min.

[17] Our conversion from wind speed to wind power using a multi-turbine curve only accounts for the reduction of the slope of the power curve at wind speeds lower than the rated wind speed and wind speeds around the cut-out speed of a single turbine. Had we used only a single turbine power curve, small changes in wind speed at wind speeds near the cut-out wind speed of the turbine would cause the wind power output data to include changes from the full output to zero. The multi-turbine power curve is a better representation of how the output of entire wind plants change at wind speeds around the cut-out wind speed. Aside from this conversion of 1-min wind speed data into 1-min wind power data our analysis does not account for the smoothing of wind power variability that occurs within a wind plant from geographic diversity. We also do not apply any alterations to the 1-min data due to the inertia of the wind turbine. Multiple sources indicate that wind turbine inertial dampening of wind speed variability impacts time-scales on the order of 20 seconds or less, but not 1-min variability (Sorensen et al., 2007; Apt, 2007).

[18] The sites where wind speeds were too low for development of wind power were E4, E7, E20, E21, and E27. Capacity factors, based on the wind speed extrapolation and power curve conversion method outlined in this section, for the excluded sites ranged from 4% to 19%. The remaining sites had estimated capacity factors that ranged from 21% to 30%. The average capacity factor across the included sites was 25%. The average wind speed and capacity factor results are included in the appendix.

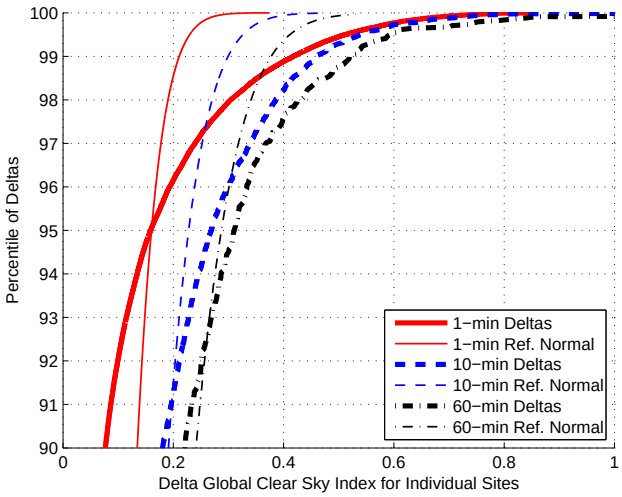

Figure 3: Cumulative probability distribution of 1-min, 10-min, and 60-min deltas of the global clear sky index at individual sites in the SGP network. The thin lines show the shape of normal distributions with similar standard deviations as the actual data.

Consistent with previous anecdotes and literature, severe deltas are apparent in the point insolation measurements from the SGP data. Large deltas greater than +/- 0.6 in the global clear sky index were observed in one minute at individual sites. Similarly, large deltas greater than +/- 0.6 were observed based on 10-min and 60-min averaging intervals (Figure 3). Figure 3 is a cumulative probability distribution plot of the deltas from the individual sites where the magnitude of the deltas are smaller than the value on the x-axis for the percent of the deltas shown on the y-axis. For reference cumulative distribution functions of normal or "bell curve" distributions with the same standard deviations as the actual 1-min, 10-min, and 60-min deltas are included as thin lines in the figure. This chart shows that extreme deltas occur very infrequently, but the shape of the distribution, particularly for the 1-min deltas, shows a higher probability of extreme deltas than would be expected for a normal distribution with a similar standard deviation. In other words, the distribution of the deltas exhibits "fat tails" relative to a normal distribution.

The standard deviation of the deltas in the global clear sky index increase with longer time scales from 1-min to 180-min (Figure 4a). The 180-min deltas have nearly double the standard deviation of the 1-min deltas. Figure 4a shows the standard deviation and 99.7^{th} percentile of the deltas averaged (but not aggregated) across the 23 sites in the SGP network. The error bars represent +/- one standard error, but are small enough to fit within the markers. The figure shows that 99.7% of the deltas are consistently below about 0.6 for 60-min and shorter deltas. For these time scales, deltas larger than 0.6 are therefore likely to occur less than 0.3% of the year. Another way to interpret these results is that for a single site, the average clear sky index over a 60-min period only has a probability of 0.3% of being 0.6 larger or smaller than the average clear sky index in the next 60-min period.

If the distribution of deltas was normally distributed, 99.7% of deltas would be within

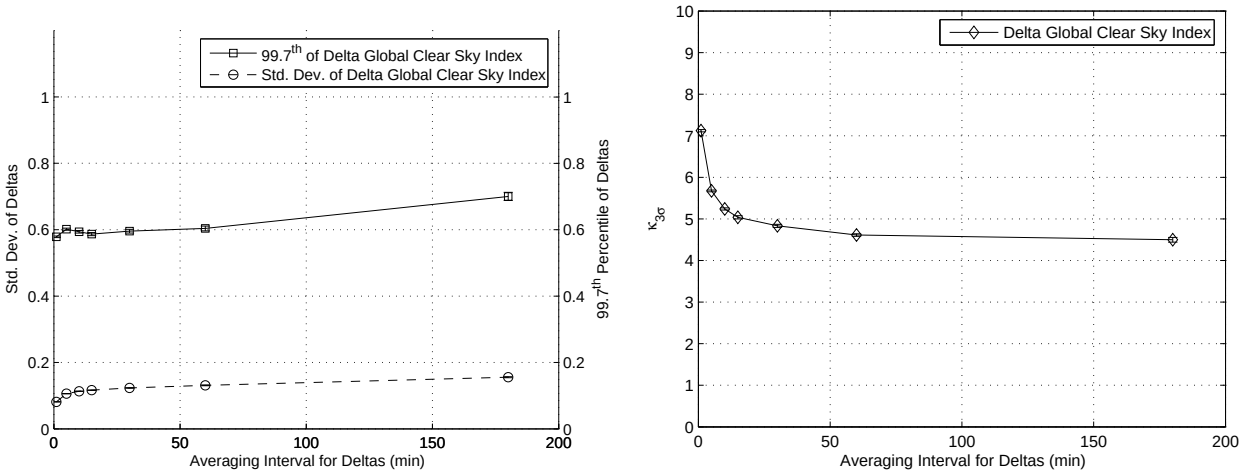

(a) Standard deviation and 99.7^{th} percentile **(b)** Ratio of 99.7^{th} percentile and standard deviation

Figure 4: (a) Standard deviation and 99.7^{th} percentile of deltas in global clear sky index over different averaging intervals for the individual sites within the SGP network. (b) The ratio of 99.7^{th} percentile and standard deviation of deltas in global clear sky index at individual sites. Error bars represent +/- one standard error from the mean (N = 23).

three standard deviations. The "fat tails" evident in Figure 3, however, lead to the 99.7^{th} percentile being much larger than three standard deviations (Figure 4b). The 99.7^{th} percentile of the 1-min deltas, for example, is seven standard deviations. The ratio is reduced for deltas over longer time scales, but even the 99.7^{th} percentile of the 180-min deltas remain more than four standard deviations, demonstrating that the distribution of the deltas with averaging intervals of 1-min to 180-min all have "fat tails" relative to a normal distribution.

The deltas at individual sites therefore demonstrate that severe changes are possible and that they occur more frequently than expected if the deltas were assumed to have the same standard deviation but be normally distributed. The balancing resources required to accommodate 99.7% of the deltas therefore exceeds that which would be required were one instead trying to manage variability based on three standard deviations. These deltas for individual sites reflect behavior similar to the assumptions used in many of the previous studies on PV integration. Jewell and Unruh (1990), for instance, simulated up to 50% changes in 1-min output from PV. The electric system modeled in that study was shown to incur inadvertent interchanges with other balancing areas if the penetration of PV was just 2% of the peak system load on a capacity basis. Assuming that the highest deltas in the SGP dataset occurred while the clear sky radiation is sufficient for a PV system to be at its rated capacity, the 1-min deltas in the SGP data could be as severe as 80% of the PV capacity were there no smoothing in the PV plant itself. Deltas above 60% of the rated capacity would be expected 0.3% time, again assuming no smoothing within the PV plant. Changes of this magnitude are found to exist over all averaging intervals from 1-min to 60-min. Such severe changes in PV output would be technically challenging and expensive to accommodate if

they did in fact occur with large scale PV deployment.

5.2 Correlation of Deltas with Distance

We now turn to a consideration of the correlation of deltas in the clear sky index across a region in order to understand the impact of aggregating the output of several PV sites. Figure 5 shows the correlation of deltas across the time-scales of 1-min to 180-min for pairs of sites at different distances from one another. In addition, the figure includes the line of best fit to Eq. 8. As shown in the figure, we find nearly zero correlation of 1-min deltas between all 23 sites in the SGP network. Even the closest sites in the network, separated by 20.5 km, demonstrate zero correlation in 1-min deltas. Similar zero correlation for 1-min deltas was found for sites as close as 2 km in Japan by Murata et al. (2009), and nearly zero correlation was found for 1-min deltas on a highly variable day for different inverters within a single 13.2 MW PV plant in the U.S. (Mills et al., 2009a). Clearly, even within a very small region 1-min deltas are nearly uncorrelated.

The near zero correlation for sites as close as 20 km was similarly found for 5-min deltas in the clear sky index. For 10-min deltas, however, a slight increase in the correlation between deltas at the closest sites becomes apparent. Hourly deltas exhibit clearer correlation between sites especially for sites that are closer than about 75 km apart. Three hour deltas are correlated for sites that are even farther apart.

Our use of the clear sky index in this case avoids an issue that is apparent in the analysis of the data used by Murata et al. (2009). Because Murata et al. (2009) use insolation or PV production data to examine the correlation of ramps with distance, the correlation between sites due to the deterministic component of the movement of the sun's position in the sky leads to correlation of ramps longer than about 15-min even for sites that are very far apart.[19] The same problem is apparent in the correlations presented by Curtright and Apt (2008). Because the clear sky index removes the influence of this deterministic portion of the data, the correlations we present in Figure 5 approach zero with increasing distance.

The near zero correlation for 1-min and 5-min deltas implies that aggregating output from PV sites at least 20 km apart[20] will smooth, as measured by the standard deviation, the 1-min and 5-min deltas by a factor of $\frac{1}{\sqrt{N}}$. Aggregating the output from sites 20 km apart will smooth deltas over longer time scales to a lesser degree than the deltas for shorter time scales due to the greater correlation of deltas with larger averaging intervals.

5.3 Aggregate Deltas from Geographically Dispersed Sites

In this section we consider the impact of aggregating geographically dispersed sites. We begin by aggregating the actual point measurements of the clear sky index from the SGP

[19]For deltas 15-min and longer, the results from Murata et al. (2009) show non-zero correlation for sites as far as 923 km apart. This is because Murata et al. (2009) include the deterministic portion of the PV output in the data used for estimating correlations.

[20]Or at least 2 km apart for 1-min deltas and 9 km apart for 5-min deltas, according to the data from Murata et al. (2009).

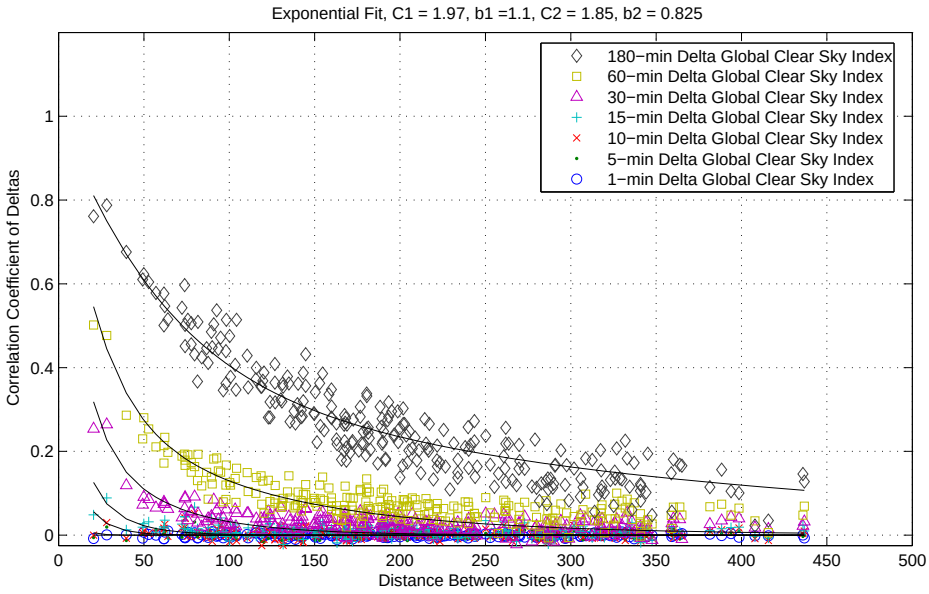

Figure 5: Correlation of changes in global clear sky index between 23 geographically dispersed solar insolation measurement sites in the SGP network. (—) Fit to the correlation data to the relationship in Eq. 8.

sites and then project the smoothing that would occur from a denser array of PV sites.

5.3.1 Smoothing from Aggregating SGP Sites

We first aggregate clear sky index data from five close sites[21] within the SGP network and then aggregate the data from all 23 sites within the SGP network.[22] Figure 6 shows an example of smoothing from averaging of the global insolation across multiple sites on a partly cloudy day. As expected, the aggregation of the simultaneous output of sites within the SGP network leads to a reduction in the *relative* magnitude of the deltas for all time scales compared to scaling the output of a single site across the entire year. This reduction in the relative magnitude of the deltas is more pronounced for all sites (Figure 8) than for five close sites (Figure 7). The distribution of the 1-min deltas from the aggregation of sites also appears to be more normal in that the tails of the distribution are less pronounced than the tails of the distribution of 1-min deltas from a single site (Figure 3). Aggregating the output from 5 close sites in the SGP network, for example, reduces the magnitude of the most extreme 1-min deltas to below +/- 0.4 from the observed +/-0.8 deltas shown for a single site in the previous section. Aggregating all 23 sites further reduces the most extreme

[21]The sites are E9, E11-13, and E15. The closest two sites are about 50 km apart. The furthest two sites are about 170 km apart. The area between the five sites is about 7,000 km^2, just larger than the state of Delaware.

[22]The 23 sites with solar data are C1,E1-13, E15, E16, E18-22, E24, and E27. The closest sites are 20 km apart and the furthest sites are 440 km apart. The area of the SGP network is around 143,000 km^2, similar in area to the states of Wisconsin, Iowa, or Illinois.

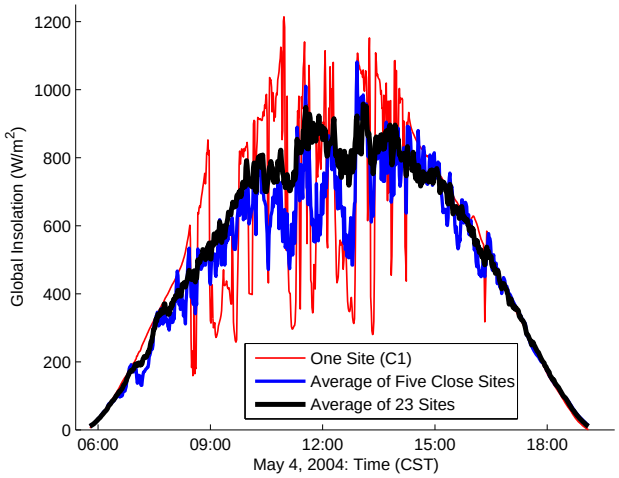

Figure 6: Example of 1-min global insolation from one site, the average of five close sites, and the average of all 23 sites in the SGP network on a partly cloudy day.

1-min deltas to below +/-0.2. Assuming that such a severe delta occurred while PV plants were at their rated capacity would lead to a maximum 20% change in the output of all PV plants in 1-min, far below the 80% change that could occur at a single site in 1-min under the same assumptions. Because the reduction in the relative magnitude of the deltas with aggregation is a key result of this analysis, we summarize the cumulative distribution of deltas from individual sites and aggregated sites for convenience in Figure 9.

The 99.7^{th} percentile and the standard deviation of the deltas for different averaging intervals is also significantly lower for the five and 23 aggregated sites (Figure 10a) than for individual sites (Figure 4a). For example, if all of the sites in the SGP network were to be aggregated, the balancing resources required to manage 99.7% of the 1-min deltas of the clear sky index would be only 16% of the resources required to manage 99.7% of the 1-min deltas if the same level of PV capacity were developed at an individual site. The ratio of the standard deviation of the 1-min deltas for an individual site to the standard deviation of the average of the aggregated 23 sites is 22%, slightly greater than the ratio for the 99.7^{th} percentiles.[23] The reduction in the 99.7^{th} percentile is larger than the reduction in the standard deviation due to the tightening of the distribution that also occurrs when aggregating the 1-min deltas (Figure 10b). While the ratio of the 99.7^{th} percentile to the standard deviation of 1-min deltas at an individual site is 7.1, the ratio of the same parameters for the aggregated sites falls to 4.9 (see Table 3). Comparison of the ratio of the 99.7^{th} percentile to the standard deviation shows that reductions in this ratio are apparent for all deltas, especially for those 60-min or shorter. The distributions remain slightly "fat-tailed" relative to a normal distribution, but

[23] As described in Section 3, the ratio of the standard deviation of the deltas from the aggregate of N uncorrelated sites to the standard deviation of the deltas from a single site is expected to be about $\frac{1}{\sqrt{N}} = \frac{1}{\sqrt{23}} = 21\%$.

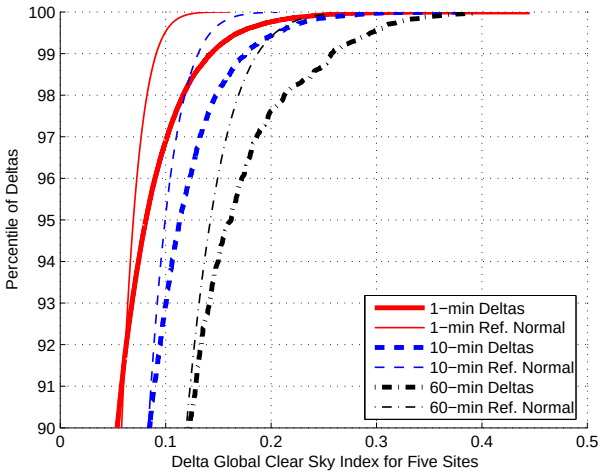

Figure 7: Cumulative probability distribution of 1-min, 10-min, and 60-min deltas of the global clear sky index for five close sites in the SGP network aggregated together (N = 5). The thin lines show the shape of normal distributions with similar standard deviations.

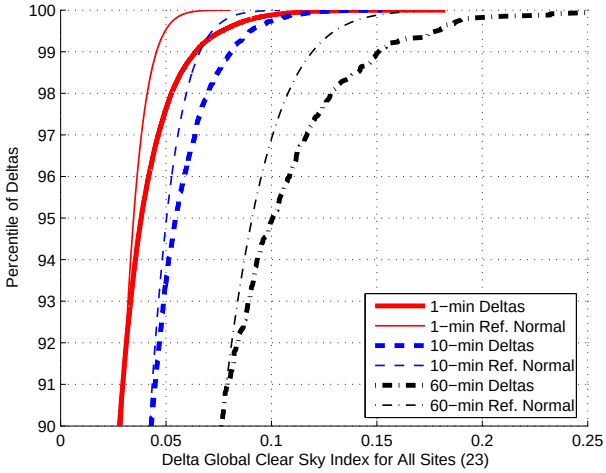

Figure 8: Cumulative probability distribution of 1-min, 10-min, and 60-min deltas of the global clear sky index for all sites in the SGP network aggregated together (N = 23). The thin lines show the shape of normal distributions with similar standard deviations.

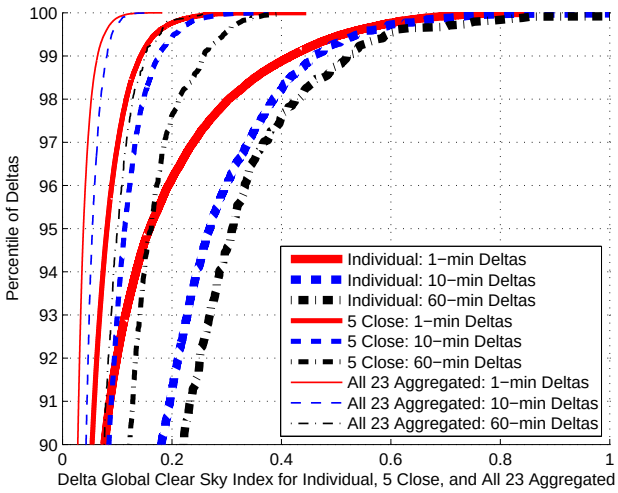

Figure 9: Cumulative probability distribution of 1-min, 10-min, and 60-min deltas of the global clear sky index for individual sites, five close sites, and all 23 sites in the SGP network aggregated together.

are much less so than for individual sites.[24]

Whereas the deltas are uncorrelated between all sites in the SGP network for time scales shorter than 5-min, Figure 5 shows that there is positive correlation for both 60-min and 180-min deltas between sites in the SGP network. Aggregating the sites that are positively correlated therefore leads to a slightly lesser benefit of geographic diversity than if all of the sites were uncorrelated. The balancing resources required to manage 99.7% of deltas from the 23 aggregated SGP sites would be 31% and 54% of the resources required to manage 99.7% of the 60-min and 180-min deltas, respectively, from an individual site (this compares to 16% for 1-min deltas, as reported earlier). The ratio of the standard deviation of the 60-min and 180-min deltas for an individual site to the standard deviation of the average of the aggregated 23 sites is 32% and 49%, respectively.

Table 3: Summary of standard deviation and 99.7^{th} percentile of global clear sky index for individual, 5 close sites, and all 23 sites in the SGP network.

	$\sigma^{\bar{t}}_{\Delta k}$			99.7^{th} percentile			$\kappa_{3\sigma}$		
Deltas	1-min	10-min	60-min	1-min	10-min	60-min	1-min	10-min	60-min
Individual Sites	0.08	0.11	0.13	0.58	0.59	0.60	7.1	5.2	4.6
5 Close Sites	0.03	0.05	0.07	0.19	0.23	0.31	5.5	4.5	4.3
All 23 Sites	0.02	0.03	0.05	0.09	0.10	0.19	4.9	3.9	4.0

[24]Slightly "fat-tailed" distributions for wind variability have also been noted (e.g. Holttinen et al. (2008)).

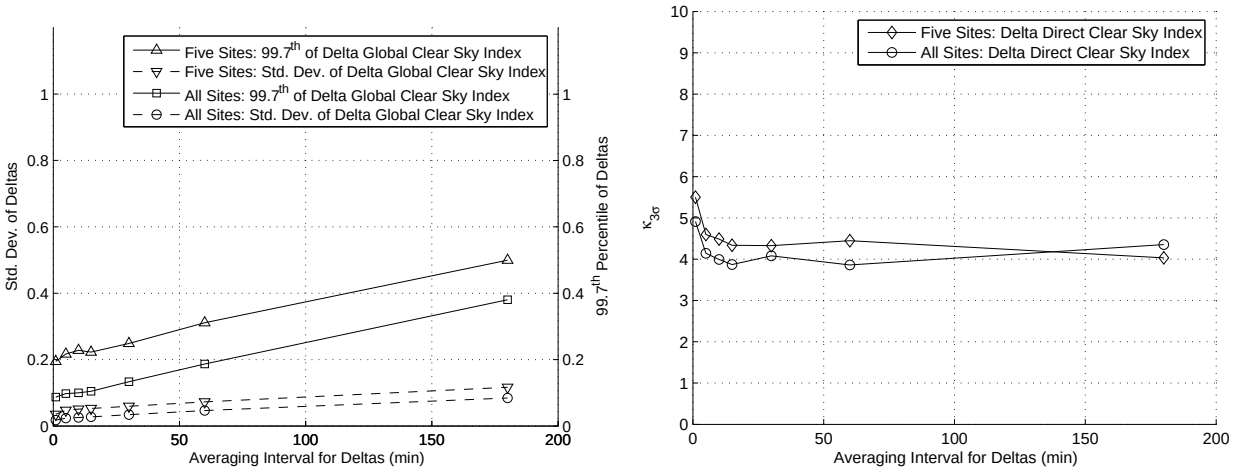

(a) Standard deviation and 99.7^{th} percentile **(b)** Ratio of 99.7^{th} percentile and standard deviation

Figure 10: (a) Average standard deviation and 99.7^{th} percentile of deltas in global clear sky index from five close sites and all sites aggregated together in the SGP network over different averaging intervals. (b) The ratio of 99.7^{th} percentile and standard deviation of deltas in global clear sky index from five close sites and all sites aggregated together in the SGP network.

5.3.2 Smoothing from a Denser Array

The area covered by the SGP network is sizable. Aggregating sites over 400 km apart to achieve the benefits of geographic diversity may not always be feasible, either because individual balancing areas are smaller than this size or because solar resource conditions or transmission costs support more dense spacing of solar plants. In this section we use the fit to the correlation of deltas with distance (Eq. 8), the deltas observed at individual sites (Figure 4a), and the "diversity filter" (Eq. 7) to predict the deltas that would be observed from aggregating a much more dense array of sites. We estimate the maximum of the 99.7^{th} percentile of deltas by conservatively assuming that the ratio of the 99.7^{th} percentile to the standard deviation of the deltas does not change relative to an individual site (see Figure 4b). This assumption is conservative since the analysis of the SGP data did show a degree of reduction in this ratio (Figure 10b) especially for shorter averaging intervals. We do not know with certainty, however, how the ratio of the 99.7^{th} percentile to the standard deviation would change for a more dense array that includes sites with deltas that are more correlated than the deltas from the sites in the more sparse SGP array.

The array that we simulate is purely to illustrate the potential broader use of the data analyzed from the SGP network. We therefore restrict the array to sites spaced by at least 20 km so that we do not need to extrapolate from the fit in Figure 5. Specifically, we use a 10×10 site square array of 100 sites spaced by 20 km on a grid.[25] As shown in Figure 11,

[25]The total area of the dense array would be 40,000 km^2, smaller than the 52,000 km^2 area of San Bernardino County, an area in Southern California with a high solar resource potential.

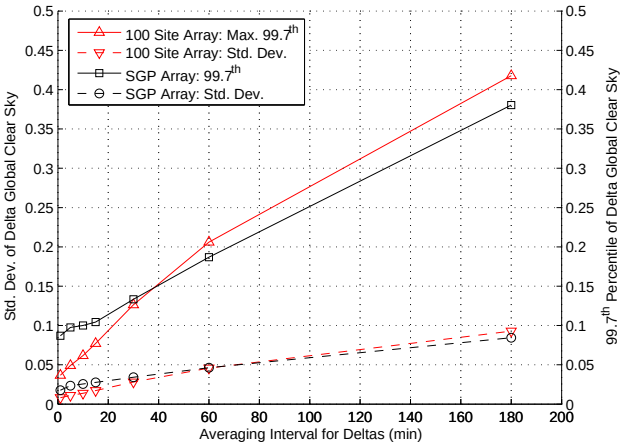

Figure 11: Comparison of the standard deviation and 99.7th percentile of deltas in global clear sky index for the individual sites within the SGP network compared to the same for a simulated array of 100 sites arranged in a more dense 10 $\times$ 10 grid with 20 km spacing between sites.

for an array with these characteristics, we find that the maximum expected 99.7th percentile of the 30-min or shorter deltas would be smaller than the deltas observed from the aggregate of the 23 sites in the SGP network. The relative aggregate variability is reduced because of the increase in the number of sites that are uncorrelated. For longer time scales, however, the close sites within the dense array are more correlated than the sites in SGP network. Over these time scales, therefore, the benefit of the greater number of sites in the dense array is balanced by the fact that the deltas of the sites are more correlated over time scales of 60-min and 180-min. As a result of the counteracting trends, Figure 11 (in comparison to Figure 4a) shows that the aggregate variability of the dense array with 100 sites is similar to the aggregate variability of the sparse SGP network with 23 sites for longer time scales.

Across all time scales, the simulated dense array requires far fewer resources to manage the aggregate variability than if the same amount of PV were to be installed at a single site with no benefit of geographic diversity. The resources required to manage 99.7% of the deltas for the dense array for time scales of 15-min and shorter are predicted to be less than 10% of the clear sky insolation, six times less than the resources required to manage the variability of the same amount of PV if all solar were to be located at a single site. The resources to manage 99.7% of the 60-min deltas for the dense array is 20% of the clear sky insolation—three times less than if the same amount of PV were based at a single site.

5.4 Comparison of Solar and Wind Deltas from Similarly Sited Plants

One way to put these results into perspective is to compare the expected variability from an array of PV sites to a similarly spaced array of wind sites. We performed a similar analysis for 1-min normalized wind power data estimated from 10 wind speed measurement sites

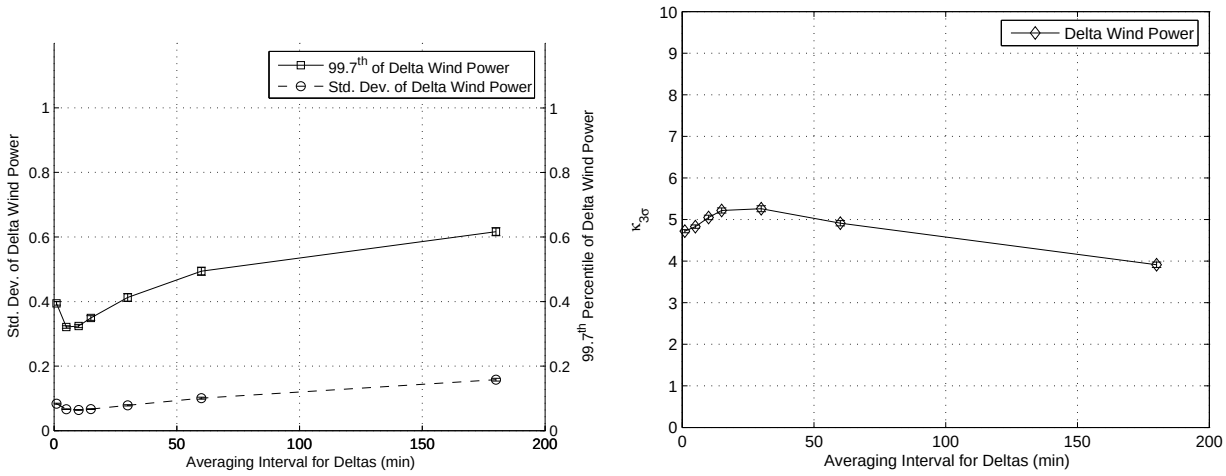

(a) Standard deviation and 99.7^{th} percentile **(b)** Ratio of 99.7^{th} percentile and standard deviation

Figure 12: (a) Standard deviation and 99.7^{th} percentile of deltas in normalized wind power over different averaging intervals for the individual sites within the SGP network. (b) The ratio of 99.7^{th} percentile and standard deviation of deltas in normalized wind power at individual sites. Error bars represent +/- one standard error from the mean (N = 10).

within the SGP network. Namely, we estimated the deltas of the normalized wind power at individual sites (Figure 12a), the ratio of the 99.7^{th} percentile to the standard deviation of the deltas (Figure 12b), and the correlation of deltas as a function of the distance between sites and the time scale of the deltas (Figure 13).

The standard deviation of 1-min deltas at individual wind sites was comparable to the 1-min deltas of the clear sky index at individual sites, but the standard deviation of deltas over longer time scales were somewhat less for the wind sites. The 99.7^{th} percentile was significantly less for wind than for solar, especially for 60-min and shorter averaging intervals. The tails of the 1-min and 5-min delta distributions were slightly less "fat" for wind than for solar (Figure 12b). The correlation of wind deltas for dispersed sites in the SGP network demonstrated similar behavior as found for solar and previous studies using actual wind turbine output in Germany (Ernst et al., 1999). Overall, however, deltas for wind were slightly more correlated than deltas for solar (the non-deterministic component measured by the clear sky index) for any given distance, particularly for deltas longer than 30-min (Figure 13). This comparison of the correlation with distance and variability at individual sites suggests that wind is less variable than solar at individual sites, but wind in this region benefits slightly less from geographic diversity than does solar.

Next we use the fit to the correlations in Figure 13 based on Eq. 8, the deltas observed at individual sites (Figure 12a) and the "diversity filter" (described by Eq. 7) to predict the deltas that would be observed from aggregating an array of wind sites for comparison to a similarly arranged array of solar sites. The array we chose for this section was again based on the constraint that we did not want to extrapolate from the data obtained from the SGP

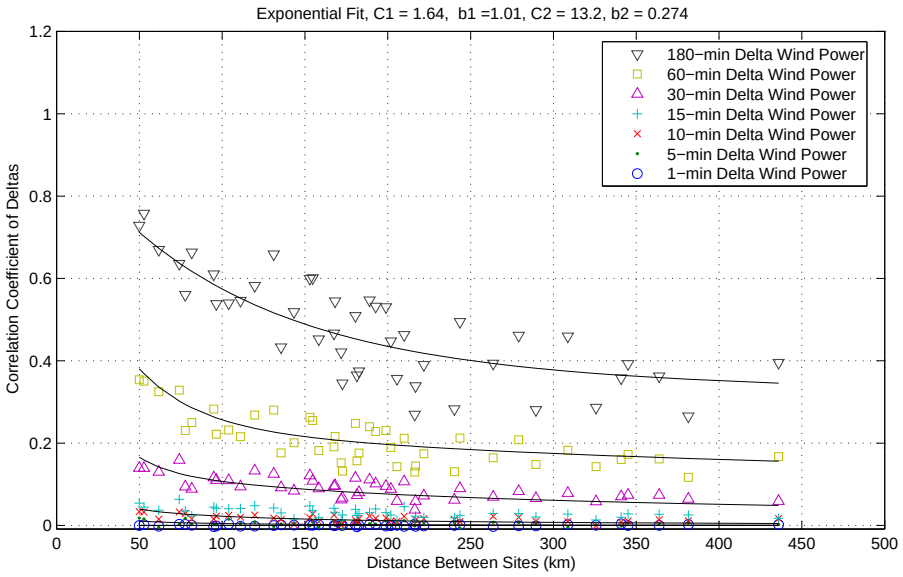

Figure 13: Correlation of changes in wind power between 10 geographically dispersed wind speed measurement sites in the SGP network. (—) Fit to the correlation data to the relationship in Eq. 8.

network. Since the closest wind measurement sites were 50 km apart, we simulate a 5 × 5 site square array of 25 sites spaced by 50 km on a grid for both solar and wind (see Figure 14 and note that the solar array included here is a different arrangement of sites than the arrays evaluated in Section 5.3). The 99.7^{th} percentile is again estimated for both solar and wind by assuming that the ratio of the 99.7^{th} percentile to the standard deviation for the array is equivalent to the ratio for a single site.

The results of this simulation demonstrate that the standard deviation of the deltas of similarly sited solar and wind plants in the 5 × 5 array are reasonably comparable, particularly for 30-min and longer deltas. The 99.7^{th} percentile of the 5 to 15-min deltas are notably smaller for wind, however. If balancing resources were procured based on the 99.7^{th} percentile, for example, the 10-min deltas for solar would require nearly double the balancing resources that wind requires.[26] The results also show for both the aggregated solar and wind, the longer time scale deltas are expected to be much larger in magnitude than the shorter time scale deltas. The 60-min deltas, for instance, are double or greater the magnitude of the 15-min and shorter deltas.

5.5 Potential Cost Impacts

Detailed studies of the changes in power system operations required to manage the short time-scale variability of PV are required to fully understand the cost implications of short-

[26]We tested a variety of different spacings for the array of sites to determine if these conclusions depended on our choice of array spacing. Although the overall shape of Figure 14 changes, the primary conclusions still hold with other array orientations.

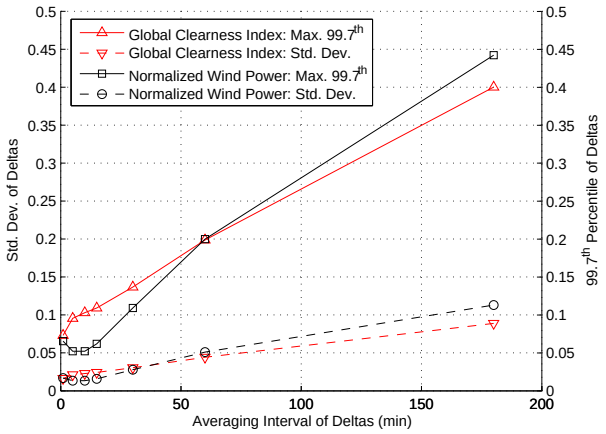

Figure 14: Comparison of the simulated standard deviation and 99.7th percentile of deltas in global clear sky index to normalized wind power from similarly arranged array of 5 $\times$ 5 grid with 50 km spacing between sites.

term PV variability. As a first approximation, however, we can use a simple method and set of assumptions to estimate the cost of managing the short time-scale variability of solar. With this simple method, we examine the relative difference in cost of managing solar all based at a single site, solar dispersed over multiple sites, and similarly sited solar and wind. Our comparison lacks any consideration of within-plant smoothing based on geographic diversity, which may be relatively more important for short time scales (1-10 min) for wind in comparison to solar due to the lower areal density of wind plants.[27] Regardless, we rely on a simple method to estimate the additional cost of holding spinning or utilizing non-spinning reserves to accommodate the short-term variability of PV and wind assuming a 10% penetration of wind or solar (on a capacity basis). These costs only address the short-term variability and do not address other costs (e.g., unit commitment costs due to day-ahead forecast errors) or benefits (e.g., capacity value and energy value) of PV.

5.5.1 Estimated Cost of Reserves

The estimated increase in the cost of balancing reserves per unit of variable generation relative to the cost of balancing reserves without variable generation is summarized in Table 4. The costs for a single site and five close sites of solar are based on the standard deviation of the deltas for the different time scales observed in Figure 4a and Figure 10a, respectively. The costs for a 25 site grid of solar and wind are based on the standard deviation of the

[27]Assuming a solar plant density of 20 W/m^2 (Denholm and Margolis, 2008), a 100 MW plant would cover an area of 5 km^2 or a square 2.2 km long on a side. Wind plant density, on the other hand, is around 5W/m^2 due to the spacing between turbines within a plant (DOE, 2008, p. 156). A 100 MW wind plant would cover an area of 20 km^2 or a square 4.4 km on a side.

deltas for the different time scales projected in Figure 14. Again, the standard deviation is used because we do not use 1-min time synchronized load data from the same region to determine the shape of the distribution of the net load deltas. The results in the four leftmost columns of Table 4 show the cost of balancing reserves assuming that, to accommodate the increase in solar or wind, system operators conservatively increase reserves at a constant level throughout the year ("Reserves Constant Throughout Year"). The column on the right shows the increase in the cost of balancing reserves for the 25 site grid of solar assuming, instead, that system operators set the additional reserves knowing that the variability of the solar output will change with clear sky insolation ("Reserves Change with Position of the Sun"). This captures the fact that system operators do not need to maintain reserves for solar at night and fewer reserves are required when clear sky insolation is low. The opportunity cost of capacity, however, is assumed to be based on only the peak net-load hours of the year and therefore does not change from hour-to-hour.

Placing all of the solar at a single point and holding reserves constant throughout the year leads to an increase in the cost of balancing reserves that is large enough to substantially erode any value of adding solar to the power system. Adding the same quantity of solar to the grid at the five locations that correspond to the five closest sites in the SGP network, however, increases the cost of balancing reserves relative to load alone by only about a quarter of the increase in costs from adding the solar at a single point. Further spreading the same quantity of solar to 25 sites in a 5 $\times$ 5 grid leads to an increase in the cost of balancing reserves that is only about 7% of the cost of adding the solar at a single site. Clearly, the number and orientation of the solar systems added to the grid will have a substantial impact on the overall increase in balancing reserves and the associated cost to manage the sub-hourly variability of PV. The earlier studies listed in Table 1 that scaled the output of single sites and found limits to the penetration of PV based on short-term variability may have come to dramatically different conclusions had they accounted for the potential smoothing effects of geographic diversity.

The cost of balancing reserves for geographically diverse solar sites is also not expected to be substantially different than the cost for similarly sited wind. The slightly greater variability of solar than of similarly sited wind for time scales shorter than 60-min projected in Figure 14 leads to a slightly greater increase in the cost of balancing reserves for solar than for wind if the increase in balancing reserves is constant throughout the year. If the required increase in balancing reserves is in proportion to clear sky insolation, however, the cost of balancing reserves for solar can be nearly identical to the cost of balancing reserves for wind. The decrease in the cost of balancing reserves when reserves are held in proportion to clear sky insolation is due to the fact that no reserves are needed for solar at night. The increased costs of balancing reserves for similarly sited solar and wind in a 5 $\times$ 5 grid are modest, but these results should be verified with more detailed solar and wind integration studies.

Table 4: Estimated unit cost of reserves to manage short-term variability

Time Scale	Increased Reserve Costs ($/MWh)				
	Reserves Constant Throughout Year				Reserves Change with Position of Sun
	Solar			Wind	Solar
	1 Site	5 Sites	25 Site Grid		
1-min Deltas	$16.7	$4.8	$1.2	$0.9	$0.8
10-min Deltas	$17.3	$4.4	$1.0	$0.2	$0.7
60-min Deltas	$5.0	$1.6	$0.6	$0.5	$0.5
Total Cost	$39.0	$10.8	$2.7	$1.6	$1.9

6 Conclusions

Our analysis demonstrates that step-changes or deltas in solar insolation at individual points can be severe. Infrequent step changes from one averaging interval to the next with averaging times from 1-min to 180-min can exceed 60% of the clear sky insolation. The distributions of sub-hourly deltas at individual sites are fat-tailed relative to a normal distribution. The 99.7^{th} percentile of the deltas, therefore, is much larger than three standard deviations.

Previous studies of the integration of PV into the electric power system demonstrate that scaling the output from an individual solar site leads to limits of the penetration of PV on the grid. The limit is due to the additional balancing resources required to accommodate the variability of PV plants, and the variability over short time scales (sub-hourly) is found to be particularly challenging to accommodate. Increasing balancing reserves to accommodate the variability of solar located at a single point is estimated to lead to a significant increase in costs and, as suggested by earlier studies, could limit the amount of solar that can be added to the power system.

As is well known for wind, however, accounting for the potential for geographic diversity can significantly reduce the magnitude of extreme deltas, the resources required to accommodate variability, and the potential increase in balancing reserve costs. The aggregate of just five close sites in the SGP network show that 99.7% of the 15-min and shorter deltas are no larger than 25% of the expected clear sky output of the aggregated sites. Furthermore, we estimate that 99.7% of the 15-min and shorter deltas from 100 sites in a 10×10 grid with 20 km spacing would be no larger than 10% of the clear sky output of the aggregated sites (this compares to 60% for an individual site). We also find that the sub-hourly deltas from similarly sited solar and wind are expected to be within the same order of magnitude, though deltas in the 5-15 min range are expected to be somewhat more severe for solar than for wind.

The cost of accommodating the short-term variability of similarly sited solar and wind

plants is expected to be comparable in this region, but further research is required to understand the costs of managing the variability and the within-plant smoothing for solar that can occur on shorter time scales. Moreover, the non-normal distribution of deltas indicate that more detailed studies may wish to focus on managing variability for a target maximum percentile (i.e., directly estimate reserves to manage the 99.7^{th} percentile events rather than assume that the distribution is normal and three standard deviations is equivalent to the 99.7^{th} percentile). Consideration of variability on time-scales of about 15-minutes or longer, meanwhile, should be careful to account for the deterministic changes in PV plant output due to changes of the position of the sun. Future studies should evaluate the spatial and temporal scales of geographic diversity in regions where PV is expected to be deployed in large quantities, particularly the desert Southwest. High time resolution (1-min or less), time-synchronized data for multiple sites separated by a distances of 2km to 200 km is required for such future work. Finally, although it was not considered in this study, studies of regions that expect both PV and wind deployment should evaluate the potential for the same balancing reserves be used to accommodate variability of both PV and wind simultaneously.

A Approximating the Cost of Balancing Reserves

In this appendix we provide details of how our estimates of the cost of balancing reserves were derived. The basic method follows an approach first described by Farmer et al. (1980), then simplified by Grubb (1991), and then applied in practice by Milborrow (2001). The objective of the analysis is to estimate the cost of providing additional balancing reserves to manage the variability of wind or solar generators at the system level per unit of variable energy generation, URC ($/MWh). The total cost of balancing reserves is assumed to be the sum of the reserves required over various time scales. Following EnerNex Corp. and Windlogics Inc. (2006), for instance, this would be the reserves based on the 1-min deltas (regulation), 5-min deltas (load following),[28] and 60-min deltas (operating reserve margin). In this appendix, we simplify the notation for the deltas by simply referring to the standard deviation of the deltas normalized by the peak as σ. Therefore, σ_L is the standard deviation of the load deltas over a particular averaging interval divided by the peak load. Similarly, σ_V is the standard deviation of the deltas of a variable generator over a particular averaging interval divided by the nameplate capacity of the variable generator. The standard deviation of the deltas from the load net variable generation normalized by the peak load (without variable generation) is σ_{L-V}.

A.1 Unit Reserve Costs of Variable Generation

For all time scales, we assume that the increase in the unit reserve costs per MWh of variable generation (URC) is the difference in the annual reserve costs for managing the net-load with variable generation (ARC_{L-V}) relative to the annual reserve costs for load alone (ARC_L) per unit of energy produced by the variable generator (E_V).

$$URC = \frac{ARC_{L-V} - ARC_L}{E_V} \tag{10}$$

The annual energy produced by the variable generator (E_V) depends on the capacity factor of the variable generator (CF_V) and can be written relative to the penetration of the variable generator on a capacity basis ($\alpha = \frac{K_V}{K_L}$) and the peak load (K_L).

$$E_V = K_L \alpha CF_V 8760 \tag{11}$$

A.2 Reserve Costs for 1-10 min Deltas

For 1-min and 10-min variability, we assume that only on-line and synchronized resources (or spinning balancing reserves) can be used to manage variability and that there is an opportunity cost of capacity that accompanies these reserves. The opportunity cost of capacity for the reserves is the unit cost of capacity, FC_p (in units of $/MW-h), multiplied by the

[28] We use the 10-min deltas in place of the 5-min deltas since the NERC CPS2 reliability performance standard focuses on 10-min averages of the area control error (ACE).

amount of balancing reserve during peak net-load hours. We assume that the amount balancing reserve is a multiple, κ, times the standard deviation of the load or net load deltas. The multiple κ is assumed to be three for both the load and the net-load, corresponding to 99.7% of the deltas if the load and net-load deltas were normally distributed.[29] While the amount of reserve procured in any hour ($\sigma_L K_L$ for load) can vary, the opportunity cost of capacity is fixed throughout the year and only depends on the amount of reserve procured during peak load periods. We always assume that even if the reserve procurement changes throughout the year, the peak reserve requirement will correspond to the peak load requirement.

The hourly cost of keeping units positioned to provide spinning balancing reserve is the product of the variable cost of the marginal unit (c_m) and the part-load efficiency penalty (η) times the amount of required spinning reserve in each hour. The part-load efficiency penalty represents the increase in the variable costs for the rest of the energy that the spinning unit generates relative to the variable cost if the plant were at its most efficient set point (generally full capacity) (see Mills et al. (2009b) for additional discussion). The amount of spinning balancing reserve in each hour is a multiple (γ) of the standard deviation of the load or net load deltas in each hour. The multiple γ is also assumed to be three for both the load and net load. The annual reserve costs to manage the 1-min or 10-min deltas for the load is then:

$$ARC_L = \sum_{8760} \eta c_m \gamma \sigma_L K_L + 8760 F C_p \kappa \sigma_L K_L \tag{12}$$

If the multiples κ and γ are assumed to be equivalent between the load and the net load (in other words if the shape of the distribution of the deltas is assumed to be the same for the load and the net load) and constant throughout the year then the unit reserve costs for the 1-min or 10-min deltas simplifies to:

$$URC = \frac{\eta c_m \gamma \frac{1}{8760} \sum_{8760} (\sigma_{L-V} - \sigma_L) + F C_p \kappa (\sigma_{L-V} - \sigma_L)}{\alpha C F_v} \tag{13}$$

Assuming that the load deltas and the variable generator deltas are uncorrelated[30] implies

[29] We know from the earlier analysis that the deltas of solar and wind are not normally distributed, but we do not know how the distribution of the load deltas will compare to the distribution of the net-load deltas. The shape of the distribution of net-load deltas may become closer or further from normally distributed than the distribution of the load deltas alone or the variable generation deltas alone. Since we do not have 1-min time-synchronized load data that corresponds to the 1-min time-synchronized solar and wind data, we cannot directly estimate the shape of the distribution of the net-load deltas. Instead, we rely on this simplifying assumption, explicitly acknowledging that this is a simple analysis and is not meant to guarantee that the result will be an accurate estimate of the cost to manage 99.7% of the deltas for the different time scales.

[30] The 60-min variable generation and load deltas are likely to be correlated to some degree. The stochastic changes in insolation due to clouds, as captured by the clear sky index, however, are less likely to be correlated with changes in load than the changes in total solar insolation and load. Either way, we do not use time-synchronized load variable generation data to account for correlation between generation and load deltas in our simple estimates. More detailed evaluations of the costs of managing short-term variability for a specific load should account for the potential correlation of generation and load over the 60-min time-scale, but

that the standard deviation of the net load normalized by the peak load (σ_{L-V}) can be calculated as:

$$\sigma_{L-V} = \sqrt{(\sigma_L)^2 + (\sigma_V \alpha)^2} \tag{14}$$

The unit reserve costs can then be simplified further to:

$$URC = \frac{\eta c_m \gamma \sigma_L \frac{1}{8760} \sum_{8760} \left[\left(1 + \left(\frac{\sigma_V \alpha}{\sigma_L} \right)^2 \right)^{\frac{1}{2}} - 1 \right] + FC_p \kappa \sigma_L \left[\left(1 + \left(\frac{\sigma_V \alpha}{\sigma_L} \right)^2 \right)^{\frac{1}{2}} - 1 \right]}{\alpha CF_v} \tag{15}$$

A.3 Reserve Costs for 60-min Deltas

In the case of the reserves used to manage the 60-min deltas we assume that both spinning and non-spinning resources can be used to meet these 60-min balancing reserve requirements. Furthermore, we again assume that there is there is an opportunity cost of capacity associated with these reserves. The total amount of balancing reserve is the multiple κ times the standard deviation of the load or net load deltas and κ is again assumed to equal three.

The variable cost of non-spinning reserves is assumed to be equal to the product of the difference between the variable cost of energy from the standing plant (c_g) and the variable cost of the marginal unit (c_m). The amount of energy that is used from the standing plant to provide energy is a multiple ($U(\gamma)$) of the standard deviation of the net load or load deltas. The multiple is called the utilization function, $U(\gamma)$, and it represents the amount of energy that is expected to come from non-spinning reserves in each hour assuming that the amount of spinning reserves is proportional to the multiple γ. The utilization function assumes that the deltas are normally distributed and is given by:

$$U(\gamma) = \int_{\gamma}^{\infty} (x - \gamma) Z(x) dx \tag{16}$$

Where $Z(x)$ is the standard normal probability density.

The ratio of the spinning reserves to non-spinning reserves depends on the relative cost of each resource. With the particular numerical assumptions we made in Table 2, the least cost way to provide reserves is to manage 0.5 times the standard deviation of the load or net-load deltas with spinning reserves ($\gamma = 0.5$ for 60-min deltas in contrast to $\gamma = 3$ when all of the balancing reserves are met by spinning reserves as assumed for 1-min and 10-min deltas) and to manage the remaining deltas with non-spinning reserves ($U(\gamma = 0.5) = 0.198$). The annual reserve costs for the 60-min load deltas is therefore:

$$ARC_L = \sum_{8760} \sigma_L K_L \left(\eta c_m \gamma + (c_g - c_m) U(\gamma) \right) + 8760 FC_p \kappa \sigma_L K_L \tag{17}$$

the correlation is not expected to be significant. The equation below can account for correlation by adding $2\rho_{L,V}\sigma_L\sigma_V\alpha$ under the square root, where $\rho_{L,V}$ is the correlation between the deltas of the load and variable generation. The other equations would need to be modified in a similar manner.

Assuming that the portion of the 60-min deltas that is met with spinning reserves (γ) is the same between the load and the net load, and that the 60-min deltas for the load and the variable generator are not correlated, leads to unit reserve costs of:

$$URC = \frac{\sigma_L \left(\eta c_m \gamma + (c_g - c_m)\, U(\gamma)\right) \frac{1}{8760} \sum_{8760} \left[\left(1 + \left(\frac{\sigma_V \alpha}{\sigma_L}\right)^2\right)^{\frac{1}{2}} - 1\right] + FC_p \kappa \sigma_L \left[\left(1 + \left(\frac{\sigma_V \alpha}{\sigma_L}\right)^2\right)^{\frac{1}{2}} - 1\right]}{\alpha CF_V} \tag{18}$$

A.4 Changing Reserves with the Position of the Sun

As operators gain more experience with solar it will be clear that the level of reserves that are needed to accommodate sub-hourly variability in the early morning, late evening, or winter months when insolation is low are not the same as the amount of reserves required to accommodate variability during summer midday hours when solar plants are near capacity. Instead of assuming that reserves are constant throughout the year, in this section we assume that reserve needs are proportional to clear sky insolation. The normalized standard deviation of the deltas of the net-load in Eq. 15 and Eq. 18 is assumed to be a time-varying quantity based on the clear sky insolation normalized by the peak clear sky insolation.

$$\sigma_V = \sigma_k \frac{G_c(t)}{G_c^p} \tag{19}$$

Where σ_k is a constant parameter throughout the year and is equivalent to the $\sigma_{\Delta k}^{\bar{t}}$ notation used earlier. Unit reserve costs are then calculated by evaluating Eq. 15 and Eq. 18 with a time series of one year of clear sky insolation. The clear sky insolation is estimated from a simple "no-sky" set of equations based on the time of year and the location using standard methods available in the "Air-sea" time-series package from the United States Geological Survey.[31] We assume that the reserves during the peak period are planned to accommodate a case where the clear sky insolation is at its maximum during the period of capacity scarcity (i.e. we assume that $\frac{G_c(t)}{G_c^p} = 1$ when estimating the capacity impacts of additional reserves in Eq. 15 and 18).

The results of this analysis are summarized in Table 4 for deltas on each time scale. The increase in the cost of reserves on each time scale is then summed to estimate the total cost of the increase in balancing reserves across all sub-hourly time scales.

[31] The matlab code for the air-sea package, developed by Bob Beardlsley and Rick Pawlowicz, is available from http://woodshole.er.usgs.gov/operations/sea-mat/.

B Estimated Capacity Factor of Modeled Wind Plants at SGP Sites

The measured 1-min wind speed data at 10-m was scaled to 80-m using a $1/7^{th}$ power law then converted into 1-min wind power data using a wind power curve. The measured wind speed, the scaled wind speed at 80-m, and the estimated capacity factor of the wind power output are summarized in Table 5. The sites where the capacity factor was less than 20% were excluded from this analysis and are not shown in this table.

Table 5: Measured wind speed at 10-m, projected wind speed at 80-m, and projected capacity factor for wind sites in SGP network

	Avg. Annual Wind Speed (m/s)		
SGP Cluster	10 m[a]	80 m[b]	Capacity Factor[c]
E1	5.05	6.79	26.4%
E3	4.53	6.10	21.3%
E5	4.59	6.17	22.2%
E6	4.55	6.13	21.2%
E8	5.47	7.36	30.4%
E9	5.29	7.12	28.5%
E11	4.65	6.25	22.8%
E13	5.39	7.25	30.0%
E15	4.71	6.34	23.1%
E24	4.77	6.42	24.7%

a - Measured wind speed
b - Extrapolated wind speed using $1/7^{\text{th}}$ power law
c - Annual average capacity factor based on 80 m wind speed data and multi-turbine power curve from Holttinen (2005)

References

Apt, J., Jun. 2007. The spectrum of power from wind turbines. Journal of Power Sources 169 (2), 369–374.

Asano, H., Yajima, K., Kaya, Y., 1996. Influence of photovoltaic power generation on required capacity for load frequency control. IEEE Transaction on Energy Conversion 11 (1), 188–193.

Beyer, H. G., Luther, J., Steinberger-Willms, R., 1990. Fluctuations in the combined power output from geographically distributed grid coupled wind energy conversion Systems-An analysis in the frequency domain. Wind Engineering 14 (3), 179–192.

Bouzguenda, M., Rahman, S., 1993. Value analysis of intermittent generation sources from the system operations perspective. IEEE Transaction on Energy Conversion 8 (3), 484–490.

Chalmers, S., Hitt, M., Underhill, J., Anderson, P., Vogt, P., Ingersoll, R., 1985. The effect of photovoltaic power generation on utility operation. IEEE Transactions on Power Apparatus and Systems PAS-104 (3), 524–530.

Chowdhury, B., Rahman, S., 1988. Is central station photovoltaic power dispatchable? IEEE Transaction on Energy Conversion 3 (4), 747–754.

Curtright, A., Apt, J., 2008. The character of power output from utility-scale photovoltaic systems. Progress in Photovoltaics: Research and Applications 16 (3), 241–247.

Denholm, P., Margolis, R. M., May 2007. Evaluating the limits of solar photovoltaics (PV) in traditional electric power systems. Energy Policy 35 (5), 2852–2861.

Denholm, P., Margolis, R. M., Sep. 2008. Land-use requirements and the per-capita solar footprint for photovoltaic generation in the united states. Energy Policy 36 (9), 3531–3543.

Doherty, R., O'Malley, M., 2005. A new approach to quantify reserve demand in systems with significant installed wind capacity. IEEE Transactions on Power Systems 20 (2), 587–595.

EnerNex Corp., Feb. 2009. Solar integration study for Public Service Company of Colorado. Tech. rep., Xcel Energy, Denver, CO.

EnerNex Corp. and Windlogics Inc., Nov. 2006. Final Report: 2006 Minnesota Wind Integration Study, Volume I. Minnesota Public Utilities Commission.

Ernst, B., Wan, Y., Kirby, B., Jul. 1999. Short-Term power fluctuation of wind turbines: Analyzing data from the german 250-MW measurement program from the ancillary services viewpoint. Tech. Rep. NREL/CP-500-26722, National Renewable Energy Laboratory, Golden, CO.

Farmer, E., Newman, V., Ashmole, P., 1980. Economic and operational implications of a complex of wind-driven generators on a power system. Physical Science, Measurement and Instrumentation, Management and Education, Reviews, IEE Proceedings A 127 (5), 289–295.

Glasbey, C. A., Graham, R., Hunter, A. G. M., 2001. Spatio-temporal variability of solar energy across a region: a statistical modelling approach. Solar Energy 70 (4), 373–381.

Gross, R., Heptonstall, P., Anderson, D., Green, T., Leach, M., Skea, J., Mar. 2006. The Costs and Impacts of Intermittency: An assessment of the evidence on the costs and impacts of intermittent generation on the British electricity network. UK Energy Research Centre (UKERC), Imperial College London.

Grubb, M., 1991. Value of variable sources on power systems. IEE Proceedings-Generation, Transmission and Distribution C 138, 149–165.

Healey, J. V., 1984. The effects of non-coherence on energy extraction from a turbulent wind. Wind Engineering 8 (4), 221–230.

Hoff, T. E., Perez, R., Oct. 2010. Quantifying PV power output variability. Solar Energy 84 (10), 1782–1793.

Holttinen, H., 2005. Hourly wind power variations in the nordic countries. Wind Energy 8 (2), 173–195.

Holttinen, H., Meibom, P., Orths, A., van Hulle, F., Lange, B., OMalley, M., Pierik, J., Ummels, B., Tande, J. O., Estanqueiro, A., Matos, M., Gomez, E., Sder, L., Strbac, G., Shakoor, A., Ricardo, J., Smith, J. C., Milligan, M., Ela, E., 2009. Design and operation of power systems with large amounts of wind power. Final Report, Phase one 2006-2008 VTT Tiedotteita - Research Notes 2493, VTT, Espoo, http://www.vtt.fi/inf/pdf/tiedotteet/2009/T2493.pdf.

Holttinen, H., Milligan, M., Kirby, B., Acker, T., Neimane, V., Molinski, T., Jun. 2008. Using standard deviation as a measure of increased operational reserve requirement for wind power. Wind Engineering 32, 355–377.

Ilex Energy Consulting Ltd, Electricity Research Centre, Electric Power and Energy Systems Research Group, Manchester Centre for Electrical Energy, Aug. 2004. Operating reserve requirements as wind power penetration increases in the Irish electricity system. Tech. rep., Sustainable Energy Ireland, Dublin, Ireland.

Ilex Energy Consulting Ltd, Strbac, G., Oct. 2002. Quantifying the system costs of additional renewables in 2020. Tech. rep., Department of Trade and Industry, Oxford, UK.

Jewell, W., Ramakumar, R., 1987. The effects of moving clouds on electric utilities with dispersed photovoltaic generation. IEEE Transactions on Energy Conversion EC-2 (4), 570–576.

Jewell, W., Unruh, T., 1990. Limits on cloud-induced fluctuation in photovoltaic generation. IEEE Transaction on Energy Conversion 5 (1), 8–14.

Kawasaki, N., Oozeki, T., Otani, K., Kurokawa, K., Nov. 2006. An evaluation method of the fluctuation characteristics of photovoltaic systems by using frequency analysis. Solar Energy Materials and Solar Cells 90 (18-19), 3356–3363.

Kern, E. J., Russell, M., 1988. Spatial and temporal irradiance variations over large array fields. In: Photovoltaic Specialists Conference, 1988., Conference Record of the Twentieth IEEE. pp. 1043–1050 vol.2.

Kirby, B., Milligan, M., 2008. An examination of capacity and ramping impacts of wind energy on power systems. The Electricity Journal 21 (7), 30–42.

Kirby, B., Milligan, M., Jul. 2009. Capacity requirements to support Inter-Balancing area wind delivery. Technical Report NREL/TP-550-46274, National Renewable Energy Laboratory, Golden, CO.

Lee, S., Yamayee, Z., 1981. Load-Following and Spinning-Reserve penalties for intermittent generation. IEEE Transactions on Power Apparatus and Systems PAS-100 (3), 1203–1211.

McNerney, G., Richardson, R., 1992. The statistical smoothing of power delivered to utilities by multiple wind turbines. IEEE Transactions on Energy Conversion 7 (4), 644–647.

Milborrow, D., 2001. Penalties for intermittent sources of energy. Working paper for the PIU energy review, London, U.K., http://www.cabinetoffice.gov.uk/media/cabinetoffice/strategy/assets/milborrow.pdf.

Mills, A., Alstrom, M., Brower, M., Ellis, A., George, R., Hoff, T., Kroposki, B., Lenox, C., Miller, N., Stein, J., Wan, Y., Dec. 2009a. Understanding variability and uncertainty of photovoltaics for integration with the electric power system. Tech. Rep. LBNL-2855E, Lawrence Berkeley National Laboratory, Berkeley, CA, http://eetd.lbl.gov/EA/emp/reports/lbnl-2855e.pdf.

Mills, A., Wiser, R., Milligan, M., OMalley, M., 2009b. Comment on Air emissions due to wind and solar power. Environmental Science & Technology 43 (15), 6106–6107.

Murata, A., Yamaguchi, H., Otani, K., 2009. A method of estimating the output fluctuation of many photovoltaic power generation systems dispersed in a wide area. Electrical Engineering in Japan 166 (4), 9–19.

Nanahara, T., Asari, M., Sato, T., Yamaguchi, K., Shibata, M., Maejima, T., 2004. Smoothing effects of distributed wind turbines. part 1. coherence and smoothing effects at a wind farm. Wind Energy 7 (2), 61–74.

North American Electric Reliabiilty Corporation (NERC), Apr. 2009. Accommodating high levels of variable generation. White paper.

North American Electric Reliability Corporation (NERC), Oct. 2008. Standard BAL-001-0.1a Real Power Balancing Control Performance. North American Electric Reliability Corporation (NERC).

Otani, K., Minowa, J., Kurokawa, K., Oct. 1997. Study on areal solar irradiance for analyzing areally-totalized PV systems. Solar Energy Materials and Solar Cells 47 (1-4), 281–288.

Persaud, S., Fox, B., Flynn, D., Nov. 2000. Modelling the impact of wind power fluctuations on the load following capability of an isolated thermal power system. Wind Engineering 24, 399–415.

Piwko, R., Clark, K., Freeman, L., Jordan, G., Miller, N., Feb. 2010. Western wind and solar integration study. Tech. rep., National Renewable Energy Laboratory, Golden, CO, http://wind.nrel.gov/public/WWIS/.

Piwko, R. J., Bai, X., Clark, K., Jordan, G. A., Miller, N. W., Jul. 2007. Intermittency Analysis Project: Appendix B: Impact of Intermittent Generation on Operation of California Power Grid. California Energy Commission, PIER Research Development & Demonstration Program.

Smith, J., Milligan, M., DeMeo, E., Parsons, B., 2007. Utility wind integration and operating impact state of the art. IEEE Transactions on Power Systems 22 (3), 900–908.

Sorensen, P., Cutululis, N., Vigueras-Rodriguez, A., Jensen, L., Hjerrild, J., Donovan, M., Madsen, H., 2007. Power fluctuations from large wind farms. IEEE Transactions on Power Systems 22 (3), 958–965.

Tovar-Pescador, J., 2008. Modelling the statistical properties of solar radiation and proposal of a technique based on boltzmann statistics. In: Modeling Solar Radiation at the Earths Surface. Springer Berlin Heidelberg, Berlin, Heidelberg, pp. 55–91.

Tuohy, A., Meibom, P., Denny, E., O'Malley, M., 2009. Unit commitment for systems with significant wind penetration. IEEE Transactions on Power Systems 24 (2), 592–601.

U.S. Department of Energy (DOE), May 2008. 20% wind energy by 2030: Increasing wind energy's contribution to U.S. electricity supply. Tech. Rep. DOE/GO-102008-2567.

U.S. Department of Energy (DOE), Forthcoming. Integration of Concentrating Solar Power and Utility-Scale Photovoltaics into Regional Electricity Markets. Washington, D.C.

Wan, Y., Dec. 2005. A primer on wind power for utility applications. Tech. Rep. NREL/TP-500-36230, National Renewable Energy Laboratory, Golden, CO.

Wan, Y., Milligan, M., Parsons, B., Nov. 2003. Output power correlation between adjacent wind power plants. Journal of Solar Energy Engineering 125 (4), 551–555.

Wan, Y., Parsons, B., Aug. 1993. Factors relevant to utility integration of intermittent renewable technologies. Tech. Rep. NREL/TP-463-4953, National Renewable Energy Laboratory, Golden, CO.

Wiemken, E., Beyer, H. G., Heydenreich, W., Kiefer, K., 2001. Power characteristics of PV ensembles: experiences from the combined power production of 100 grid connected PV systems distributed over the area of germany. Solar Energy 70 (6), 513–518.

Wiser, R., Bolinger, M., Aug. 2010. 2009 Wind technologies market report. Tech. Rep. DOE/GO-102010-3107, National Renewable Energy Laboratory, Golden, CO.

Woyte, A., Belmans, R., Nijs, J., Feb. 2007. Fluctuations in instantaneous clearness index: Analysis and statistics. Solar Energy 81 (2), 195–206.